

UC San Diego

UC San Diego Electronic Theses and Dissertations

Title

A High Precision Method to Measure Neon Isotope Fractionation at the Firn-to-Ice Transition on Polar Ice Sheets

Permalink

<https://escholarship.org/uc/item/34f8q6mx>

Author

Liang, Christy

Publication Date

2018

Peer reviewed|Thesis/dissertation

UNIVERSITY OF CALIFORNIA SAN DIEGO

**A High Precision Method to Measure Neon Isotope Fractionation
at the Firn-to-Ice Transition on Polar Ice Sheets**

A thesis submitted in partial satisfaction of the
requirements for the degree Master of Science

in

Earth Science

by

Christy Yafen Liang

Committee in charge:

Jeffrey P. Severinghaus, Chair
Ralph Keeling
Jane Teranes

2018

Copyright

Christy Yafen Liang, 2018

All rights reserved.

The thesis of Christy Yafen Liang is approved, and it is acceptable
in quality and form for publication on microfilm and electronically:

University of California, San Diego

2018

TABLE OF CONTENTS

Signature Page	iii
Table of Contents	iv
List of Figures	vii
List of Tables	ix
Acknowledgements	x
Abstract of the Thesis	xii
1. Introduction	1
1.1. Motivation	1
1.2. Why Neon?	2
1.3. Main Challenge	4
1.3.1. Argon interference in mass spectrometer	4
1.4. General information about the air samples	6
1.4.1. Standard air	6
1.4.2. Sample air	6
2. Overview of Method	8
2.1. Method in general	8
2.1.1. Vacuum line	8
2.1.1.1. 5 Å molecular sieve	9
2.1.1.2. Helium as the carrier gas	9
2.1.2. Mass spectrometer	10
2.2. Predicted results and precision	11
2.3. Method requirements	12
3. Method development – pure gases	14
3.1. Mass spectrometer capability	15
3.1.1. Pure neon gas	15
3.1.2. Neon and helium mixture	16
3.2. Neon and 5 Å molecular sieve	17
3.3. Separation of neon and argon	18

3.4. Thermal fractionation	21
3.5. Argon chemical-slope.....	23
3.6. Mathematical corrections	26
3.6.1. Pressure imbalance correction.....	26
3.6.2. Doubly-charged ^{40}Ar on singly-charged ^{20}Ne isobaric interference correction	27
3.6.3. Doubly-charged $^{44}\text{CO}_2$ on singly-charged ^{22}Ne isobaric interference correction ..	28
3.6.4. Ricochet $^{28}\text{N}_2$ on ^{22}Ne interference correction	28
3.7. Results after correction.....	29
3.8. Discussion	30
4. Method development – air extraction	31
4.1. How to remove most of the air?	32
4.1.1. Does removing air quickly fractionate neon isotope?	35
4.2. La Jolla air as the standard	36
4.2.1. Timing of mol-sieve in liquid nitrogen	37
4.3. Surface Greenland air	40
4.4. Discussion: Why does surface Greenland air \neq La Jolla air?	41
4.4.1. Incomplete transfer?	41
4.4.2. Problem caused by the additional water trap?	42
4.4.3. Leak in from room air neon on the vacuum line or mass spectrometer?	43
4.4.4. Is there neon contamination from the ultra-pure helium?	45
4.4.5. Insufficient mathematical corrections?.....	47
5. Method development – second attempt of air extraction	51
5.1. Adjustment for the second attempt.....	51
5.2. Exact Mathematical corrections	52
5.2.1. Pressure imbalance correction.....	52
5.2.2. Ricochet $^{28}\text{N}_2$ on ^{22}Ne interference correction	53
5.2.3. Doubly-charged $^{44}\text{CO}_2$ on singly-charged ^{22}Ne isobaric interference correction ..	53
5.2.4. Doubly-charged ^{40}Ar on singly-charged ^{20}Ne isobaric interference correction	54
5.3. La Jolla air as the standard	55
5.4. Surface Greenland firm air	57
5.5. Discussion: Why SGA \neq LJA?.....	57
5.5.1. Different pressure and vessel?.....	57
5.5.2. Thermal expansion?	58
5.5.3. Mass spectrometer changed?.....	58

6. Conclusion	59
6.1. Achievements	59
6.2. Next attempt	59
7. Appendix.....	60
7.1. Derivation of simple approximations in the same correction order of pure gases experiments	60
7.2. Derivation of more precise corrections in the same order of section 5.....	62
References.....	68

LIST OF FIGURES

Figure 1: Schematic of mass and size dependent fractionation of gases during bubble close-off in polar ice. Neon isotope measurements can provide some insights about mass-dependent fractionation at the transition zone.....	3
Figure 2: Neon isotope measurements using two pure neon standard cans. Error bars show the standard deviation from the mean of the 26 aliquots, which is 0.011 ‰. The mass spectrometer can measure neon with high precision.....	15
Figure 3: Schematic of a standard can connected to a bellow in the mass spectrometer.	16
Figure 4: Neon isotope measurements of replicate aliquots from two standard cans with neon and helium mixture. Error bars show the standard deviation from the mean of the 20 aliquots, which is 0.010 ‰. The mass spectrometer can measure a lower amount of neon when sufficient carrier gas is added.....	17
Figure 5: Comparison of neon transfer with and without 5Å mol-sieve. Using mol-sieve does not cause fractionation.....	18
Figure 6: Schematic of neon and argon separation procedure. Pure neon and argon are added to the vacuum line. Then the mixture is exposed to the mol-sieve to remove argon and passed through LN ₂ trap to remove any potential existing CO ₂ and water vapor. The remaining gas is collected by a dip-tube and the removal process is repeated. Lastly, helium is added to the tube to increase the gas volume. More details are described in the text above.....	20
Figure 7: Schematic of how thermal fractionation test is setup on the mass spectrometer. Two temperature sensors (red x) are placed in between two valves (green dot) on both the sample tube and the standard can.....	22
Figure 8: $\delta^{22}\text{Ne}$ deviation from the average due to temperature differences between sample and standard side. The low R-squared shows that there is no clear correlation between temperature and the observed $\delta^{22}\text{Ne}$ values.....	22
Figure 9: Comparison of Ar chemical slope generated from different procedures. a) Ar chemical slope for a single Ar removal step, and a double Ar removal. b) Zoom-in of Ar chemical slope for the double Ar removal.....	25
Figure 10: Corrected values for one and two Ar removal methods. Two Ar removal steps removes most of the argon and gives higher precision.....	30
Figure 11: Schematic of the extraction line modification throughout the method development with a pressurized cylinder of LJA. First, we added gettering to the neon extraction method (red box 2 replaced red box 1). Then, we switched to using mol-sieve only when we found out that gettering is not necessary (blue box 4 replaced blue box 3).....	34
Figure 12: Comparing the neon isotope measurements of the pure neon and the neon after mol-sieving nitrogen. Trapping nitrogen with mol-sieve does not cause measureable neon fractionation.....	36

Figure 13: Corrected $\delta^{22}\text{Ne}$ of LJA. The average is -0.035 ‰ and the external precision is 0.06 ‰..... 37

Figure 14: Ar chem-slope for different separation timings. 10 minute mol-sieving gives the best slope for precise Ar interference correction..... 39

Figure 15: Corrected $\delta^{22}\text{Ne}$ for different timings with their corresponding Ar chem-slopes. The external precision is 0.103 per mil for 20 min; 0.072 per mil for 15 min; and 0.06 per mil for 10 min. 39

Figure 16: Schematic of method development using LJA from the pier and similar setup for Greenland firn air. Dry LJA from pressurized cylinder is replaced by LJA from the pier (red box 2 replaced red box 1). One flask of LJA air is measured several times by expanding it to a smaller volume. When we switched to Greenland firn air samples, a water trap was added because the field collection process did not eliminate water vapor (red box 3 replaced red box 2).40

Figure 17: Delta values of the surface firn air plotted vs. transfer time. 41

Figure 18: Zoom-in of both tests, Ne Leak Test 4 and 5. This magnetic field v. intensity scan only shows mass 20 to mass 22. There is no detectable room neon leaking into the vacuum lines while transferring..... 44

Figure 19: Comparison of $\delta^{22}\text{Ne}$ with different equilibration times on sample side. There is no detectable effect of room neon leaking in through o-ring while equilibrating gases in the bellows of the mass spectrometer..... 45

Figure 20: The magnetic v. intensity scan of the commercial high purity helium gas tank. The ultra-purity helium gas tank is pure enough that adding helium to the samples will not affect neon isotope measurements. 46

Figure 21: The combined effect of modified correction order and calculation. Both calculations begin with PIS corrected $\delta^{22}\text{Ne}$ from the left but differ in order for argon, carbon dioxide and nitrogen interferences. The old corrections give $\delta^{22}\text{Ne}$ heavier than the modified ones..... 49

Figure 22: Comparison of how two different correction methods affect $\delta^{22}\text{Ne}$. For 10 replicates, the older method gives average of -0.83‰ and precision of 0.122‰, and the modified calculation method gives average of -0.35‰ and precision of 0.023‰..... 50

Figure 23: Ar chem-slope for exact corrections. The slope is 0.0144..... 52

Figure 24: Results of LJA. a) Raw and Corrected La Jolla Air. b) Expanded y-axis to show the corrected La Jolla Air in detail. The exact mathematical corrections have improved the external precision and satisfy the requirement of 0.03 ‰. (n = 10, mean = -0.35, σ = 0.023‰)..... 56

LIST OF TABLES

Table 1: Volume details of the double-valve dip tube and the space into which the gas sample expands, including the dip-tube and each component on the mass spectrometer, during the 10 min. homogenization.....	21
Table 2: Collected ions of neon isotopes, nitrogen, argon, and carbon dioxide in voltage from the magnetic v. intensity scan of Figure 20. This table provides quantitative evidence to prove the ultra-purity helium gas is sufficiently clean to use.	46

ACKNOWLEDGEMENTS

I would like to acknowledge support from National Science Foundation for funding the REU program at Scripps Institution of Oceanography (SIO). Thanks are due to Jane Teranes, SURF program director, for inviting me to join this program. Jane has been helpful since I began my student career at SIO. She has a wide range of understanding about various research projects at SIO and provides useful suggestions when I face difficulties. She always encourages me and supports me when I doubt myself. I also would like to acknowledge Jeffrey Severinghaus, my principal investigator, for providing this challenging and interesting project. He was willing to teach me the basics of lab work when I first began the project. He is patient when I need him to explain the same questions again, and lead me through the thinking process step by step, which trains and encourages me to think critically. This project would not have begun in 2015 and continued until now without these two mentors.

I want to acknowledge all of the members of the Severinghaus lab through the years I have been here. Berni Bereiter provided some technical help and suggestions when I first started in summer 2015. Sarah Shackleton, Alan Seltzer and Benni Birner provided creative ideas and potential solutions when I struggled with puzzling results. Jessica Ng and Jacob Morgan gave useful suggestions for my thesis writing. I would like to give thanks to our lab technician, Ross Beaudette, for all of his technical help. He not only taught me a lot about the mass spectrometer and vacuum lines, but also encourages me to think critically, so that I eventually am able to work independently. Although they were all busy, they were all willing to spare some time and their contribution help make this method development project successful.

I would like to thank Ralph Keeling for giving me the opportunity to be a volunteer and exploring gas related research because I probably would not be involved in gas related research

had I not volunteered in his lab 2014-2015. Also I thank him for serving on my committee and providing guidance when needed. I want to thank all of the members of the Keeling lab, especially Sara Afshar and Adam Cox who mentored me when I worked in the lab. I also want to thank Bill Paplawsky for all of the technical help. He is the most knowledgeable person I have ever met about electronics. I learned a lot from him.

I would also want to acknowledge help from three other colleagues at SIO, Christina Harth, Jennifer Benavides and Jinliang Gao. Christina Harth is knowledgeable about molecular sieve, and had provided many useful suggestions when we had trouble with using molecular sieve. Jennifer Benavides and Jinliang Gao are my friends who encouraged and supported me when I faced difficulties.

Finally, I want to acknowledge my family for all of their support. Although my parents do not always understand what I do and why I insist on majoring in Earth Science, they respect my choice and provide financial support whenever needed. I would not have high achievements if they did not send me to study abroad in the United States ten years ago. My twin sister, Heidi, was often the only person to consult with when I faced difficulties. Lastly, I want to thank my boyfriend and now my fiancé, Aaron, who accompanied me through my most difficult times and always encourages me to be confident. I am thankful for his understanding and support throughout the past five years.

ABSTRACT OF THE THESIS

A High Precision Method to Measure Neon Isotope Fractionation at the Firn-to-Ice Transition on Polar Ice Sheets

by

Christy Yafen Liang

Master of Science in Earth Science

University of California, San Diego, 2018

Jeffrey P. Severinghaus, Chair

Atmospheric gases and their isotopes are crucial to understanding biogeochemistry, and trapped air in ice cores affords a unique extension of atmospheric records back into the past. However, certain gases become fractionated during the bubble close-off process due to leakage from overpressured bubbles. Therefore, a detailed understanding of the leakage mechanism during this process is crucial to making corrections to measured past atmospheric isotope ratios in glacial ice. Neon isotope measurements are proposed for making such corrections for two main reasons. First, the isotopic ratio is constant in the atmosphere, so any observed changes of the ratio represent only the effect of the bubble close-off process. This can be useful for making corrections to dioxygen and dihydrogen isotope measurements. Second, the neon atom is smaller

than the critical size (3.6 Å) of the opening in the ice lattice, so quantifying neon isotopes can test and verify the widely adopted velocity-dependent hopping theory, which predicts that the light isotope should diffuse faster through the ice lattice due to its higher velocity. Although helium isotopes clearly show this effect, neon can provide insight about observed mass-dependent fractionation of other gases and its puzzling absence in argon. The newly developed neon extraction method and the first high-precision neon isotope ($^{22}\text{Ne}/^{20}\text{Ne}$) measurements have been successfully made with La Jolla air. Greenland firn air measurements will be next, which will quantify the mass-dependent gas loss at the firn-to-ice transition and can help improve the correction that is used for past atmospheric content reconstruction.

1. Introduction

1.1. Motivation

Atmospheric gases and their isotopes are crucial to understanding climatology and biogeochemistry, and trapped air in ice cores affords a unique extension of atmospheric records back into the past (Craig and Chou 1982; Etheridge et al. 1996; Barnola et al. 1987; Bender, Sowers, and Brook 1997). However, certain gases, such as oxygen (O_2), nitrogen (N_2), and some noble gases become fractionated during the bubble close-off process due to leakage from overpressured bubbles at the close-off depth, where firn turns into ice (Severinghaus et al. 2003; Huber et al. 2006; Battle et al. 2011). Consequently, the gas remaining in the ice core is not a direct measurement of what was in the air, and the fractionation process causes complications in reconstruction of the past atmosphere. In particular, oxygen is one of the important gases in ice core studies because oxygen in the past atmosphere can provide constraints on carbon dioxide fluxes (Battle et al. 1996). In addition, the O_2/N_2 ratio from ice cores can provide information about past changes in total biomass on Earth (Keeling, Piper, and Heimann 1996). Furthermore, oxygen isotopes of O_2 and hydrogen isotopes of H_2 would reveal biogeochemical processes that have relevance to understanding Earth's response to warming in the immediate future (Severinghaus et al. 2009). In order to measure these ratios precisely enough to shed light on these processes, it is essential to make accurate corrections to the measurements of the fractionated gases trapped in bubbles in ice cores in order to get the true values of past atmospheric composition.

1.2. Why Neon?

Previous attempts at using argon isotopes and Ar/N_2 to reconstruct atmospheric O_2/N_2 from the gas bubbles in the ice cores were not successful due to the limited understanding of size-dependent and mass-dependent fractionation of argon and oxygen in the ice lattice (Kobashi, Severinghaus, and Kawamura 2008). Neon will provide more insights about size-dependent and mass-dependent fractionation because of its size and inert gas properties. Observation shows that all three gases, argon, oxygen, and neon, have size-dependent fractionation at the bubble close-off depth, and neon is fractionated more dramatically (Battle et al. 2011). Since the neon atom is smaller than the critical size (3.6 Å), neon permeates through the ice lattice via velocity-dependent hopping between sites (Ikeda-Fukazawa, Kawamura, and Hondoh 2004; Severinghaus and Battle 2006). This theory predicts that the lighter isotope will diffuse faster through the ice lattice due to its higher velocity, but such mass-dependent fractionation has never been experimentally verified and quantified. A deeper understanding of this theory will provide more insights about why this particular type of mass-dependent fractionation occurs in oxygen but not argon (Ikeda-Fukazawa, Kawamura, and Hondoh 2004; Battle et al. 2011; Severinghaus and Battle 2006). One proposed hypothesis is that the mass-dependent fractionation may be related to whether the gas is monatomic or diatomic (Battle et al. 2011). Thus, neon isotopic measurement has been proposed to resolve this question because it is smaller than the critical size and it is a monatomic gas like argon (Figure 1). Additionally, neon concentration and its isotopic ratio in the atmosphere do not change significantly over time, so any observed change in ice cores must be due to the bubble close-off process at the firn-to-ice transition zone, after correction for known gravitational and thermal fractionation.

High precision neon isotopic ratio measurements for firn air have not been done in the

past because the main challenge was to separate two noble gases, argon and neon. This separation is needed because some argon-40 ions will become doubly-charged in the mass spectrometer and interfere with the neon-20 ion measurements. The purpose of this thesis is to develop a method to extract neon gas from air, whilst removing most of the argon and accounting for other possible interferences. The ultimate result of firm air neon isotope ratio measurements at different depths will help to quantify mass-dependent fractionation in the ice lattice at the firm-to-ice transition, and can help improve the correction that is used for past atmospheric content reconstruction.

Dependence of bubble close-off fractionation on molecular size

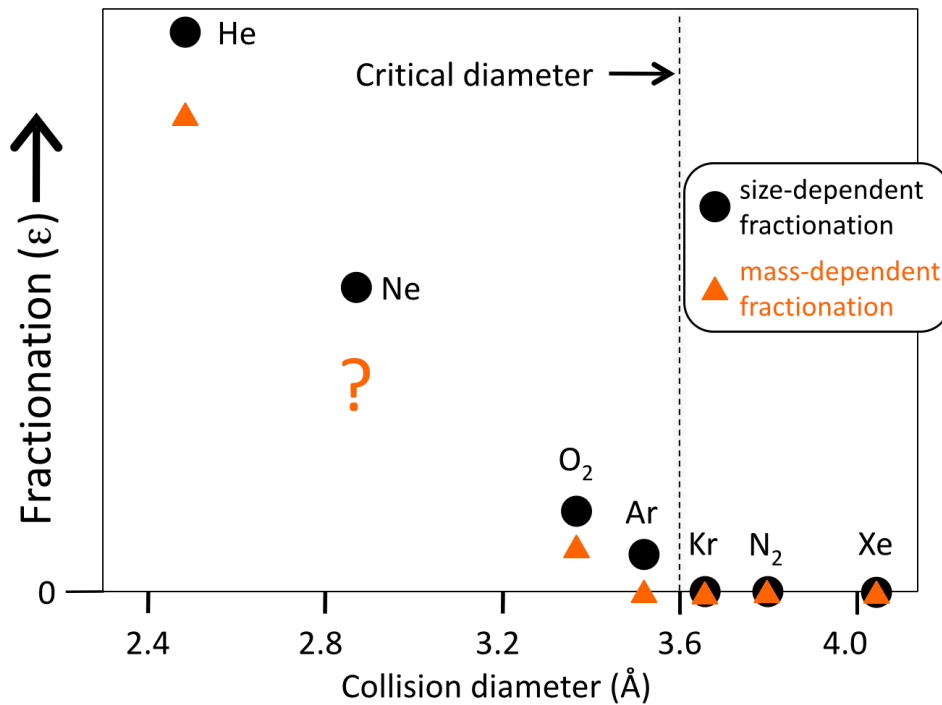


Figure 1: Schematic of mass and size dependent fractionation of gases during bubble close-off in polar ice. Neon isotope measurements can provide some insights about mass-dependent fractionation at the transition zone.

1.3. Main Challenge

1.3.1. Argon interference in mass spectrometer

Most of the noble gas extraction methods in the Scripps Noble Gas Isotope Laboratory require “gettering”, which is the process of removing all reactive gases by adsorption to zirconium-alloy sheets. Therefore, it might be expected that the neon extraction method will also use gettering. However, gettering does not eliminate argon, the most troubling gas for neon measurements, because it is also a noble gas. In the MAT 253 mass spectrometer, a higher electron energy is needed to ionize neon than argon, so when the electron energy is tuned for neon measurements, some ^{40}Ar can become doubly charged ($^{40}\text{Ar}^{++}$). $^{40}\text{Ar}^{++}$ ions cause isobaric interference with singly charged ^{20}Ne ions ($^{20}\text{Ne}^+$), because the mass spectrometer separates and collects ions into the Faraday cups according to the mass to charge ratio. This ^{40}Ar interference causes the measured $\delta^{22}\text{Ne}$ to be more negative. Consider the following equation:

$$q = \frac{\left(\frac{22}{20}\right)_{SA}}{\left(\frac{22}{20}\right)_{ST}} = \frac{\left(\frac{^{22}\text{Ne}^+ + \alpha_{N_2} \ ^{28}\text{N}_2^+ + ^{44}\text{CO}_2^{++}}{^{20}\text{Ne}^+ + ^{40}\text{Ar}^{++}}\right)_{SA}}{\left(\frac{^{22}\text{Ne}^+ + \alpha_{N_2} \ ^{28}\text{N}_2^+ + ^{44}\text{CO}_2^{++}}{^{20}\text{Ne}^+ + ^{40}\text{Ar}^{++}}\right)_{ST}} \quad (1)$$

where q is the ratio of neon isotope measurements on the sample side to the standard side ($\delta = q - 1$), “22” represents all the ions that are collected by the ^{22}Ne Faraday cup: $^{22}\text{Ne}^+$, $^{28}\text{N}_2^+$, and $^{44}\text{CO}_2^{++}$, “20” represents all the ions that are collected by the ^{20}Ne Faraday cup: $^{20}\text{Ne}^+$, $^{40}\text{Ar}^{++}$, SA means the sample side, and ST means the standard side.

If argon is not completely removed and some of the argon is ionized into doubly charged ions, the denominator of the sample side will increase, which cause $(22/20)_{SA}$ to decrease, and q will decrease. Then according to the definition of delta, $\delta^{22}\text{Ne}$ will be more negative.

$$\delta^{22}\text{Ne} \equiv (q - 1) \times 1000\text{‰} \quad (2)$$

On the MAT 253, the fraction of ^{40}Ar that becomes doubly charged is unknown and can vary depending on the state of the mass spectrometer. We released commercially-made pure argon into the mass spectrometer to estimate this fraction, so the signal measured in the $^{20}\text{Ne}^+$ cup is mostly $^{40}\text{Ar}^{++}$. The ratio of the measured ion current of $^{40}\text{Ar}^{++}$ to $^{22}\text{Ne}^+$ is about 7:1. We used this information to make an approximate argon interference correction temporarily until we got an “argon chemical slope”, which will be discussed in section 3.5. The formulas are shown below:

$$\delta^{22}\text{Ne}_{\text{Ar_artifact}} \approx \left[\left(\frac{1}{1 + \frac{1}{7} \left(\frac{^{40}\text{Ar}_{SA}^+}{^{22}\text{Ne}_{SA}^+} \right)} \right) - 1 \right] \times 1000\text{‰} \quad (3)$$

$$\delta^{22}\text{Ne}_{\text{Ar_corr}} = \delta^{22}\text{Ne}_{\text{PIS_corr}} - \delta^{22}\text{Ne}_{\text{Ar_artifact}} \quad (4)$$

$\frac{^{40}\text{Ar}_{SA}^+}{^{22}\text{Ne}_{SA}^+}$ is the raw ratio of mass 40 and mass 22 ions measured independently by varying the magnet (“peak-jumping”). In all of the air samples, nominal mass 20 ions include both $^{40}\text{Ar}^{++}$ and $^{20}\text{Ne}^+$, so $^{22}\text{Ne}^+$ is measured instead as the reference isotope needed to normalize the argon beam for bellows pressure variations. This strategy is made viable by the fact that neon isotope ratio variation is small compared to the Ar/Ne variation.

In addition, the abundance of Ar is 0.93% and Ne is 0.0018% in air, and Ar is 6 times more easily ionized than Ne in our mass spectrometer. If Ar were not removed from the sample, Ar ions would be about 3000 times more abundant than Ne ions. From the experiments on the MAT 253, we obtain a ratio of doubly charged argon ions to singly charged neon ions of 70 to 1, which means that the true signal from neon-20 would be swamped and we would need to make unworkably large corrections. Therefore, eliminating most of the argon is necessary.

1.4. General information about the air samples

1.4.1. Standard air

I need an unchanging reference as the primary standard gas for air measurements, and the modern atmosphere meets this need, because neon isotopes in the atmosphere do not change measurably on the relevant timescales (Ozima and Podosek, 2002). This modern air will be called La Jolla Air (LJA) because it is taken at the end of the pier at the Scripps Institution of Oceanography (SIO) in La Jolla.

The pier air sampling method is similar to that developed earlier in the Scripps Noble Gas Isotope Lab (Orsi PhD thesis 2013), except that the air is flushed through a 2L flask for 10 minutes. The process is always conducted in the shade to avoid thermal fractionation due to solar heating. It begins with pumping unpolluted air from over the ocean through an aspirator pump and two glass traps with beads, immersed in a mixture of ethanol and liquid nitrogen at a temperature of -80°C to -100°C to freeze out water vapor. Then the air continues through a neoprene diaphragm pump at 4L/min and through a 2L glass flask to flush clean, unfractionated air through the flask. After flushing the flask for 10 minutes, all the pumps are turned off and we wait 5 seconds before closing the two valves on the 2L flask, to avoid the fractionation that comes from closing valves on a flowing air stream. The connecting tubing between each component is made of $\frac{1}{4}$ inch synflex and various types of ultra-torr with viton o-rings.

1.4.2. Sample air

The firm air samples were collected at the “Carbon-14 camp” led by Vasilii Petrenko at Greenland summit in 2013. Air was pumped through an inflatable bladder when drilled to the desired depths, which were from the surface to the lock-in zone at about 80 m, and collected in

pre-evacuated 35L Essex tanks. Details about the Summit firm air (SFA) sampling equipment and method are recorded in Summit Field Report 2013.

Section 2 is a general discussion of how we extract neon and measure neon isotopes. It also includes our prediction of neon isotope fractionation magnitude and the goal of this method in terms of experimental precision.

Section 3 begins with pure gas experiments to avoid possible complications from using air. The preliminary method is developed at this stage along with the simple corrections for raw neon isotope measurements.

Section 4 presents the neon extraction method for air samples, and the raw neon isotope measurements are corrected with the simple mathematical corrections established with the pure gas experiments. The air extraction method is developed after the neon isotope ratio from the air of the current atmosphere is successfully measured, and the value obtained is used to normalize firm air measurements to the modern atmosphere, which is the primary standard. Some Greenland surface air samples are measured and the result will be discussed. At the end of this section, improvements on the mathematical corrections are discussed and an illustration of their effects on the raw measurements is shown.

Section 5 shows the result of the adjusted neon extraction method with improved mathematical corrections for the standard air and Greenland air.

Section 6 concludes the achievements of this research project and what can be done next.

Section 7 is the appendix that provides the derivation of the interference corrections for the raw neon isotope measurements. It includes both the simple and the more precise corrections, and an illustration of how do they affect the raw measurements.

2. Overview of method

2.1. Method in general

The following method was developed and implemented at the Noble Gas Isotope Laboratory of Professor Jeffrey Severinghaus at the Scripps Institution of Oceanography (SIO). In general, there are three phases: (1) use pure gases to demonstrate sufficient mass spectrometry precision to probe any possible fractionation caused during air extraction in the vacuum line and handling error, (2) develop a method with additional steps to extract neon from the isotopic standard, the modern atmosphere in La Jolla, CA, and (3) measure firn air samples from Greenland, collected in 2013, to use neon isotopes to learn about the physics of the bubble close-off process. This thesis will present a complete method for measurements of La Jolla air and any adjustments necessary for future Greenland firn air measurements.

2.1.1. Vacuum line

Gas extraction is performed on a vacuum line system with a turbo molecular pump and fore-vacuum pump as backup. The processed gas samples are collected in a dip-tube with cryopumping in liquid helium (LHe) at 4K. The system is built with stainless steel tubing and Swagelok SS-4H valves to regulate the gas flow. MKS Baratron manometers or MKS Convectron vacuum gauges measure pressure in different parts of the vacuum system. Ultra-torr connectors with o-ring seals and VCR Metal Gasket Face Seal fittings are used to connect different parts of the vacuum line.

2.1.1.1. 5 Å molecular sieve

One of the key materials used to carry out the neon extraction method is molecular sieve (mol-sieve), which is a synthetic zeolite with micropores that only allow selected sizes and shapes of molecules to be adsorbed. Mol-sieve is used because we want to physically separate two inert gases, argon and neon, since they cannot be separated chemically. A 5Å mol-sieve is chosen because it can trap argon and N₂, but not neon, at 77K in liquid nitrogen (LN₂) (Barrer and Robins, 1953). Removal of argon is crucial for high-precision neon measurements because the presence of argon will interfere with the neon isotope ratio measurements in the mass spectrometer (see section 3.3.1). Although mathematical corrections can be made for the interference (see section 3.6 and 4.4), the ideal approach is to remove as much argon as possible to minimize the correction magnitude and hence its contribution to the total error.

2.1.1.2. Helium as the carrier gas

To purify the air samples for neon isotope measurements, the method needs to eliminate other gases in each sample aliquot. The composition of the firn air samples from Greenland is very similar to the air in the atmosphere, so after removing most of the other gases, such as water vapor, nitrogen, oxygen, and argon, only a small amount of gas will remain. With such a small air sample, the gas flow mechanism would be molecular flow in the capillaries of the mass spectrometer, and severe neon isotope fractionation would happen. To ensure high precision neon isotope measurements, a carrier gas is added to each sample to keep the neon flow through the capillaries of the mass spectrometer inlet as a viscous flow. We chose helium as the carrier gas because helium has a very low ionization efficiency, and thus does not compete strongly with neon for electrons in the mass spectrometer source. Also, other commonly used carrier gases,

such as argon and nitrogen, would interfere with neon measurements on the mass spectrometer, which will be discussed in section 3.3 and 3.6.

2.1.2. Mass Spectrometer

Neon isotopes are measured by a dual viscous-inlet Finnigan MAT 253 mass spectrometer, which is tuned to be able to measure ^{20}Ne and ^{22}Ne beams simultaneously. In the mass spectrometer, all gases are ionized into positive ions by electron bombardment in the ion source and are accelerated into different Faraday cups based on their different mass-to-charge ratios. The collected ion currents are measured as voltages across a resistor, which are then converted in δ values by the following equation:

$$\delta = \left(\frac{R_{\text{sample}}}{R_{\text{standard}}} - 1 \right) \times 1000\text{‰} = (q - 1) \times 1000\text{‰} \quad (3)$$

where R_{sample} is the isotope ratio of the sample and R_{standard} is the ratio of the standard

$$\text{and } R = \frac{\text{Voltage of heavy isotope}}{\text{Voltage of light isotope}} \quad (4)$$

and q is the ratio of the sample over the standard.

Therefore, the neon isotope ratio measurement is reported by $\delta^{22}\text{Ne}$, and it is calculated as

$$\delta^{22}\text{Ne} \equiv \left[\frac{\left(\frac{^{22}\text{Ne}^+}{^{20}\text{Ne}^+} \right)_{SA}}{\left(\frac{^{22}\text{Ne}^+}{^{20}\text{Ne}^+} \right)_{ST}} - 1 \right] \times 1000\text{‰} \quad (5)$$

The raw $\delta^{22}\text{Ne}$ values measured by the mass spectrometer are not the true $\delta^{22}\text{Ne}$ values of the gas because they are affected by 1) pressure imbalance of the two bellows, 2) doubly-charged isobaric interference of $^{40}\text{Ar}/^{20}\text{Ne}$ and $^{44}\text{CO}_2/^{22}\text{Ne}$, and 3) ricochet interference of $^{28}\text{N}_2/^{22}\text{Ne}$ ratios. Mathematical corrections of these effects are required after the mass spectrometry and will be further discussed in Sections 3.6 (for the initial interference correction method) and 4.4

(for the improved correction method).

Every aliquot of a gas sample is associated with one $\delta^{22}\text{Ne}$ value. Each $\delta^{22}\text{Ne}$ value is the average of multiple individual measurements (typically 16 to 80) called “cycles”, which consist of measuring the sample and the standard side ratios once (Eq3). Each aliquot of gas sample is measured for at least 16 cycles, and the integration time in each cycle of measurement is 16 seconds. During the method development phase, most of the standard gases were working standards, which are made in the lab from various sources of commercially-obtained neon, and their isotopic composition can vary for different experiments, so the $\delta^{22}\text{Ne}$ absolute values are somewhat arbitrary. For this reason, we will report the result of each experiment as the $\delta^{22}\text{Ne}$ values’ deviation from the average of each set of data, until we determine the $\delta^{22}\text{Ne}$ of the ultimate working standard versus the primary standard (which is the atmosphere). Throughout the method development, the external precision, which is the standard deviation of replicate aliquots, is more meaningful than the delta value because it informs the reproducibility of the method.

2.2. Predicted results and required precision

One ultimate goal of the newly developed neon isotope analytical method is to use high precision neon isotope measurements to make corrections for bubble close-off fractionation (Severinghaus and Battle, 2006) of the isotopes of O_2 from air bubbles in ice cores. To be useful for this purpose, a certain level of precision of the neon isotope method is required, and this level is estimated here. This estimation is based on the observed magnitude of the signal of O_2 isotopic fractionation in firn air (Battle et al., 2011), and the expected fractionation of neon isotopes due to their fractional mass difference. The isotopic fractionation signal of O_2 is 5.8 ‰

and the experimental precision is about 0.003 ‰ (Battle et al., 2011). Neon is predicted to permeate through the ice lattice via a velocity-dependent process, therefore, the neon fractionation factor (α) is governed by $\sqrt{\text{mass}} = \sqrt{22/20} \approx 1.048$, so the fractionation (ϵ) is $\alpha - 1 = 48 \text{ ‰} \approx 50 \text{ ‰}$. Since the signal of neon isotope fractionation is about ten times that of O_2 , we can tolerate about ten times more experimental error for neon isotopes. Hence, the required external precision of the neon isotope measurements should be about 0.03 ‰ or less.

2.3. Method requirements

We need to meet several requirements before the method development can begin. Throughout the entire project, we need to make sure there is no leak of room air neon into the vacuum line or the mass spectrometer, nor any detectable amount of neon in the commercially-made Ultrapure helium tank that can change the sample's neon isotope composition when helium is added. Leaks generally allow the lighter isotope into the vacuum line preferentially, due to effusion fractionation through a small orifice having a diameter less than the mean free path of the neon atoms (Graham's Law). This type of fractionation is strong for neon, in principle equal to 1 minus the square root of the mass ratio $\sqrt{20/22} \approx 46 \text{ ‰}$. For example, if 1% of the measured sample came from room-air neon that had leaked in, the bias in the sample could be as much as -0.46 ‰, which is 15 times larger than our target precision.

Similarly, the trace neon that is sometimes present in commercially-obtained gases is often highly isotopically-fractionated, probably because gas purification is done by boiling off the gases from liquefied air, and the boiling point of each isotope is slightly different. For example, we measured substantial neon in a tank of commercially-obtained nitrogen, and it was

highly isotopically-fractionated. Our experiments with our tank of Ultrapure helium did not reveal any detectable neon.

In addition, we need to confirm that we collect all of the neon in the sample tube at 4 K, which means we get complete (quantitative) transfer of neon to the dip-tubes. Incomplete transfer generally results in strong isotopic fractionation, in our experience, due to the fact that heavy isotopes preferentially fail to make it to the dip-tube during the cryopumping step. These conditions are necessary for each extraction, to ensure we are measuring the true neon isotope value from each aliquot of gas sample.

3. Method development – pure gases

In the first stage of method development, we want to start with experiments using pure gases to simplify any possible complications from using air. Our goal is to find out if it is possible at all to get 0.03 ‰ external precision on the mass spectrometer under the most ideal conditions. If it is possible, then we can move to the next step and ask if the same level of external precision is possible when all the complexities of the extraction process are added. The method will not be useful if the external precision under ideal conditions is not 0.03 ‰ or less, and we would not continue in this case.

In general, the method includes two aspects, the mass spectrometer and the extraction system. For the mass spectrometry, we need to make sure that we can measure neon isotopes without artifactual (man-made) fractionation. For this purpose, we use a relatively large amount of pure neon to find out how well the neon isotopes can be measured, and then as a second step we measure the mixture of helium and neon gas to probe whether a much smaller amount of neon, as we will obtain from gas samples, can still be measured precisely when helium is added as a carrier gas.

Once we know how well the mass spectrometer can measure neon isotopes, we next test out whether the 5Å molecular sieve fractionates the neon isotope ratio, and whether neon isotope ratio measurements depend on the temperature difference between the sample and the standard side (due to thermal fractionation). These are necessary to confirm first in order to continue the development of the extraction method. Next, experiments with pure neon and argon are tested to probe the method of separating them with the mol-sieve in the extraction line. Lastly, the method cannot perfectly remove all of the unwanted gases, so small mathematical corrections are derived and applied to the measured neon isotope values to get the true ones.

3.1. Mass spectrometer capability

3.1.1. Pure neon gas

The very first step is to verify that the mass spectrometer is capable of measuring neon isotopes with high precision. The highest possible external precision on this particular mass spectrometer at its current state during method development can be found by measuring two standard cans with pure neon against each other. One aliquot of neon gas from each standard can is introduced and measured by the mass spectrometer. In Figure 2, each $\delta^{22}\text{Ne}$ is the average of 32 cycles of measurements from an aliquot, and the external precision of the 26 aliquots is 0.011 ‰. The result is better than the targeted precision of 0.03 ‰, so the mass spectrometer is functioning well and the method development can begin.

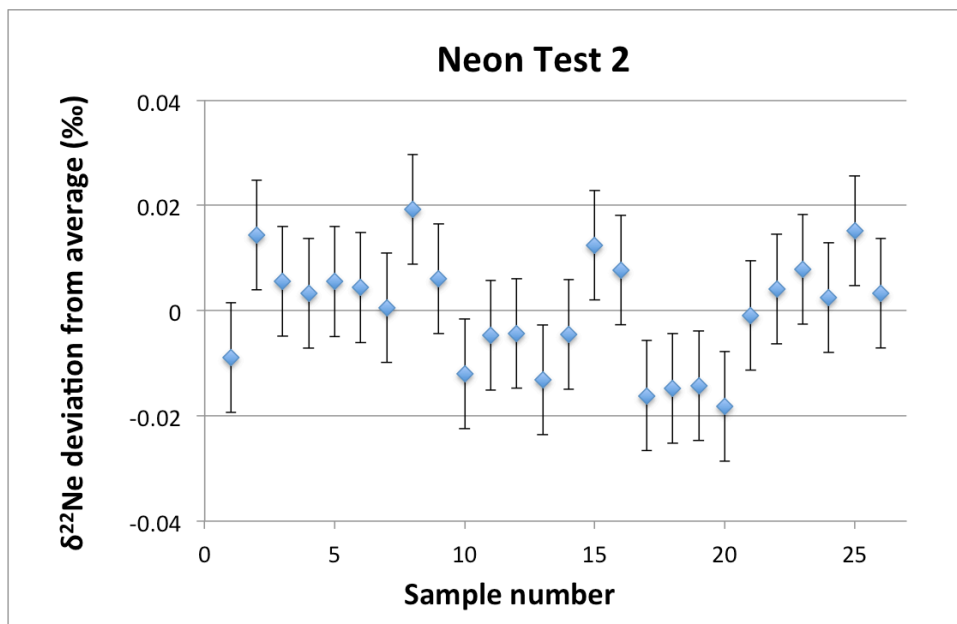


Figure 2: Neon isotope measurements using two pure neon standard cans. Error bars show the standard deviation from the mean of the 26 aliquots, which is 0.011 ‰. The mass spectrometer can measure neon with high precision.

3.1.2. Neon and helium mixture

In this step we are measuring two standard cans with a representative neon-helium mixture against each other on the mass spectrometer to determine the best possible external precision. Each standard can contains 10 torr of neon and 2000 torr of helium, and each aliquot is from the 1.3 cm³ volume between the two valves on the can (Figure 3). The outer valve is closed and the inner valve is opened, and each aliquot is taken by closing the inner valve quickly after equilibrating for 5 minutes. The aliquot is then released (expanded) into the bellows of the mass spectrometer and allowed to equilibrate for another 10 minutes. Each $\delta^{22}\text{Ne}$ value is the average of 80 cycles of measurements and the external precision of 20 repeated aliquots is 0.010 ‰ (Figure 4). The precision is similar to the pure neon (section 3.1), which shows that the mass spectrometer can measure a lower amount of neon at the same level of precision when we add helium, the carrier gas, which is necessary to avoid molecular flow regime fractionation.

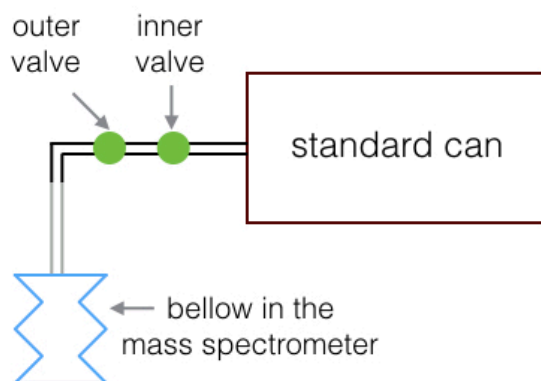


Figure 3: Schematic of a standard can connected to a bellow in the mass spectrometer.

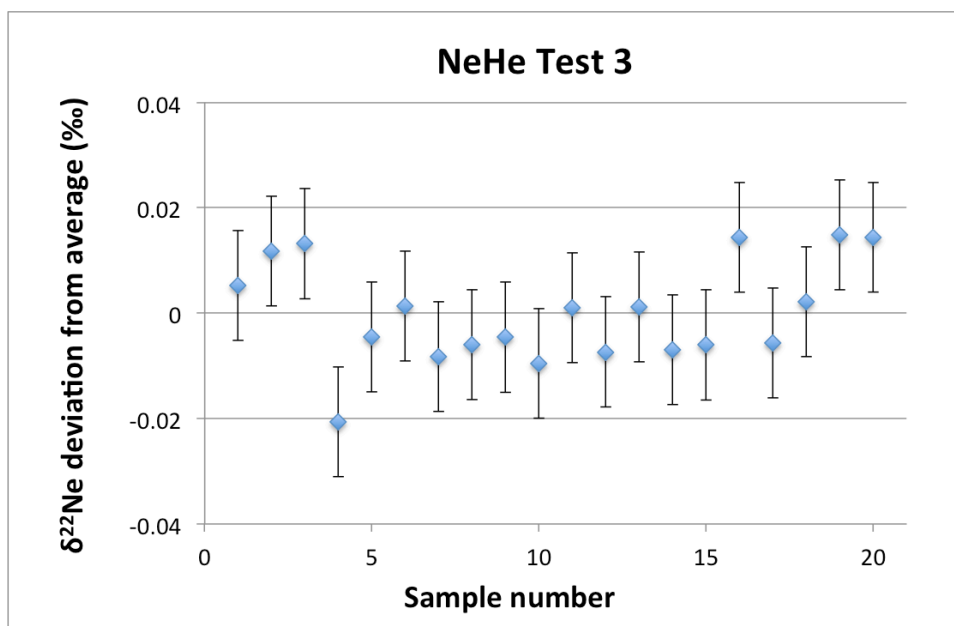


Figure 4: Neon isotope measurements of replicate aliquots from two standard cans with neon and helium mixture. Error bars show the standard deviation from the mean of the 20 aliquots, which is 0.010 ‰. The mass spectrometer can measure a lower amount of neon when sufficient carrier gas is added.

3.2. Neon and 5 Å molecular sieve

The 5Å mol-sieve is used to separate argon and neon in our method, so it is important to find out whether using the mol-sieve will cause neon isotope fractionation when separating argon and neon. For example, neon might be slightly retained by the mol-sieve, and the heavy isotope would be preferentially retained. Pure neon from a standard can is used in the two sets of experiments, one without using mol-sieve and one with mol-sieve in LN₂ during the extraction process (Figure 5). The average $\delta^{22}\text{Ne}$ without mol-sieve is -0.645 ‰ and the standard deviation is 0.052 ‰. The average value with mol-sieve is -0.661 ‰ and the standard deviation is 0.051 ‰. There is no clear pattern or distinct difference seen between these two sets of data, thus there is no evidence of detectable neon fractionation caused by mol-sieve at in LN₂ 77K.

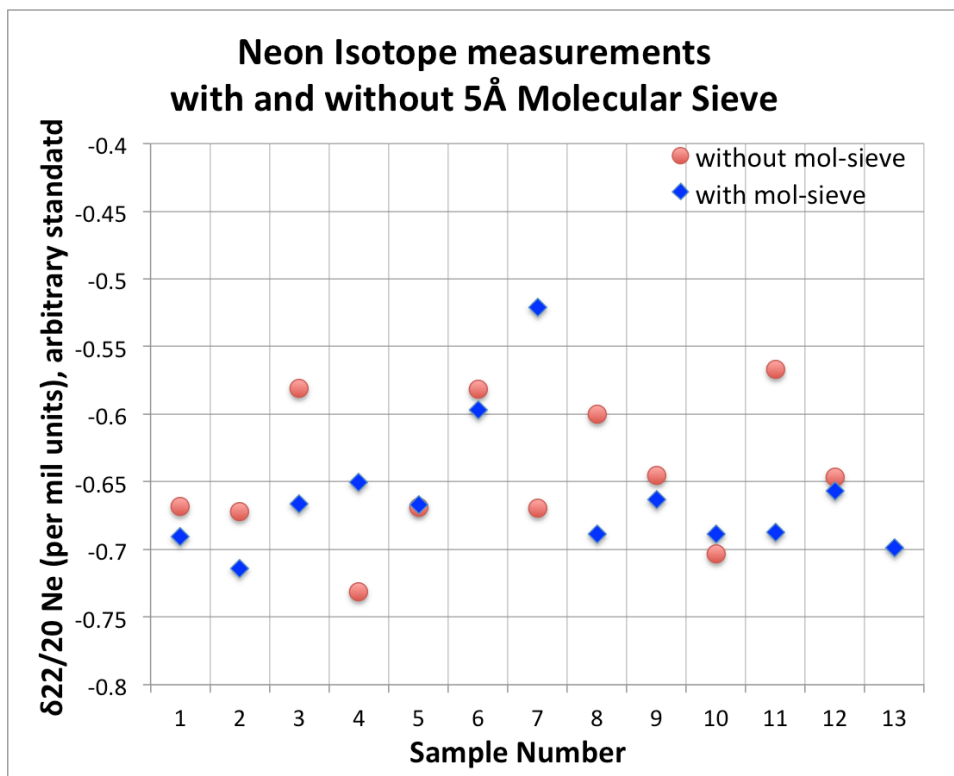


Figure 5: Comparison of neon transfer with and without 5Å mol-sieve. Using mol-sieve does not cause fractionation.

3.3. Separation of neon and argon

The separation process of neon and argon operates on a vacuum system, and a schematic is shown below (Figure 6). Before separating neon and argon, we added a fixed amount of commercial pure argon and pure neon into an isolated space in the vacuum line to obtain a mixture. We started the separation by exposing the mixture to the mol-sieve and slowly raising a dewar of LN₂ at 77K to remove argon by adsorption to the cooled mol-sieve. The remaining gases were then passed through a water trap at 77K to freeze out water vapor and carbon dioxide, and the remainder was frozen into a single-valve dip tube (dip tube 1) at 4K in liquid helium.

The Ar removal process happens quickly within several minutes, and we suspected that some neon could be trapped in the mol-sieve by the mass action of argon atoms flowing quickly

toward the adsorption sites. To get all of the neon transferred quantitatively to dip tube 1, we closed all the valves and released all the gases from the mol-sieve by taking off the liquid nitrogen and then replacing it. The liquid nitrogen was put back on when the baratron gauge showed a number close to the original gas pressure, so that any neon trapped in the mol-sieve would be released. We then repeated the cryopumping of neon to the same 4 K dip tube. This additional step minimizes the risk of neon fractionation, because neon that was trapped by the mol-sieve will have another opportunity to be transferred into the same dip tube as the sample.

Afterwards, leftover (residual) gases were evacuated through the waste pump and dip tube 1 was placed above the valve (Figure 6.) near the mol-sieve for a second argon removal step and trapping. The CO₂ and water vapor trapping was repeated again, and the remaining gases were trapped into a double-valve dip tube (dip tube 2). There was much less total gas in this second separation, as most of the argon had been removed in the first separation stage; this means neon was unlikely to be trapped by mass action in the mol-sieve during the second separation, so no release and re-trapping of argon was done.

Finally, helium carrier gas was added into dip tube 2 to increase the gas volume for the mass spectrometer measurements. We found that helium addition has to be a separate step done at room temperature after transferring neon on the vacuum line, because helium cannot be frozen into the dip tube at 4 K. Also, we found that adding a known pressure of helium gas to the neon while the dip tube was at 4 K was not workable, because the amount of helium captured in the tube can vary depending on the temperature of the dip tube, which in turn depends on the level of liquid helium in the dewar, so we were not able to add a precise and consistent amount.

In addition, we found that a double-valve dip-tube is necessary to permit addition of helium into a separate volume, between the two valves, which is later allowed to mix with the

neon. With only a single valve on the dip-tube, we found that some neon diffused out of the tube and fractionated the sample, during the addition of helium gas to the dip tube.. At room temperature, 1300 torr of helium is added into the space between two valves of the dip tube, which has a volume of 0.721 cm³.

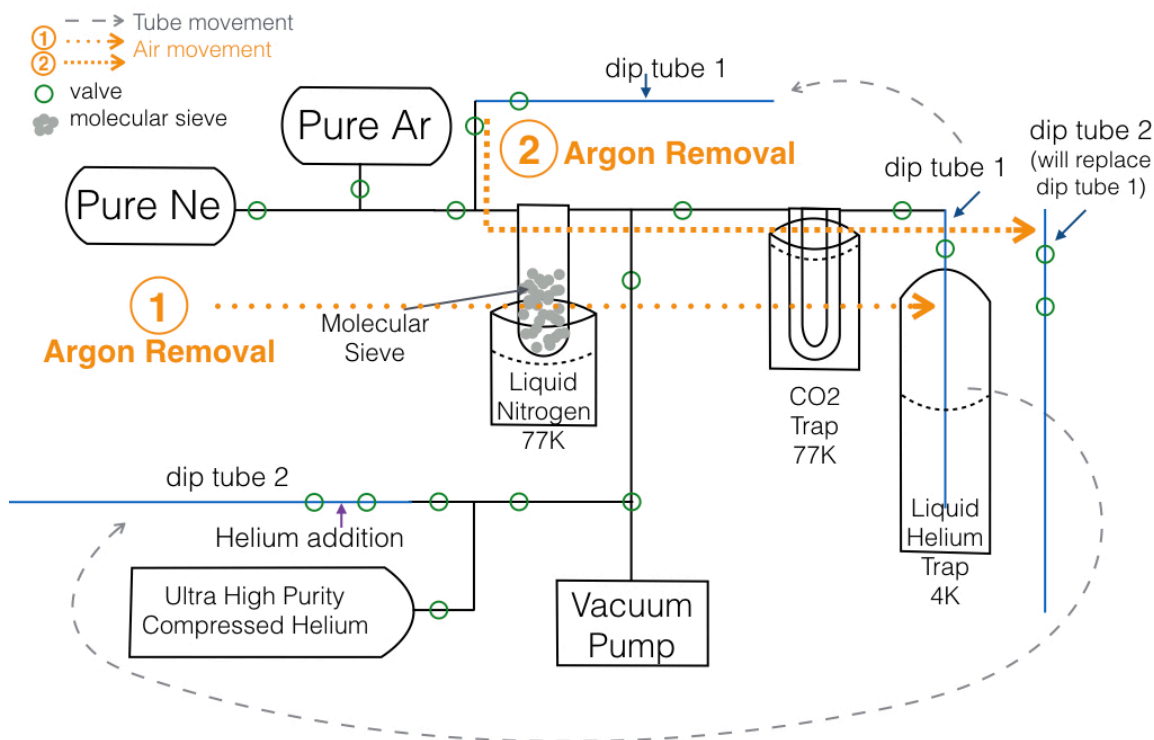


Figure 6: Schematic of neon and argon separation procedure. Pure neon and argon are added to the vacuum line. Then the mixture is exposed to the mol-sieve to remove argon and passed through LN₂ trap to remove any potential existing CO₂ and water vapor. The remaining gas is collected by a dip-tube and the removal process is repeated. Lastly, helium is added to the tube to increase the gas volume. More details are described in the text above.

After the mixture of helium and neon is homogenized, it is released into the fully expanded bellows on the sample side of the mass spectrometer and left for 10 min to equilibrate. The bellows' volume is approximately 40 cm³, the double-valve stainless steel dip tube's volume

is approximately 24.93 cm³, and the volume of the connection tubing between the dip tube and the bellows is approximately 6.70 cm³. When the gas expands into the bellows, only ~66% of the sample makes it into the bellows for measurement (Table 1). This rather large loss of sample has important implications for potential thermal fractionation, as discussed below.

Table 1: Volume details of the double-valve dip tube and the space into which the gas sample expands, including the dip-tube and each component on the mass spectrometer, during the 10 min. homogenization.

	Length (cm)	Diameter (cm)	Area (cm ²)	Volume (cm ³)
Tube	104.14	0.53	0.22	22.91
Space between valves	4.34	0.46	0.17	0.72
Valve (internal)				1.3
	Total volume of the tube is (Tube + Rotating Female Union + 2 Valves)			24.93
Connection between The tube and bellow	30	0.53	0.22	6.70

3.4. Thermal fractionation

Another important detail to know is whether there is any thermal fractionation happening when releasing the sample and standard aliquots into the mass spectrometer. We measured the temperature difference between sample and standard sides by putting a temperature sensor in between the two valves of the double-valve tube on the sample side, and in between the two valves of the standard can, where an aliquot is taken (Figure7). Each $\delta^{22}\text{Ne}$ is the average of 32 cycles of measurements and is corrected for doubly-charged Ar, doubly-charged CO₂ and N₂ ricochet interferences (these will be discussed in section 3.6), so we can see the thermal diffusion effect on the neon isotope ratio measurements, if any. Then we plot the temperature difference against the $\delta^{22}\text{Ne}$ subtracted from the average $\delta^{22}\text{Ne}$, to see if there is any obvious correlation

(Figure 8). We do not see a strong correlation between temperature difference and $\delta^{22}\text{Ne}$. Also, the R^2 is close to zero, so we conclude that there is no significant thermal fractionation.

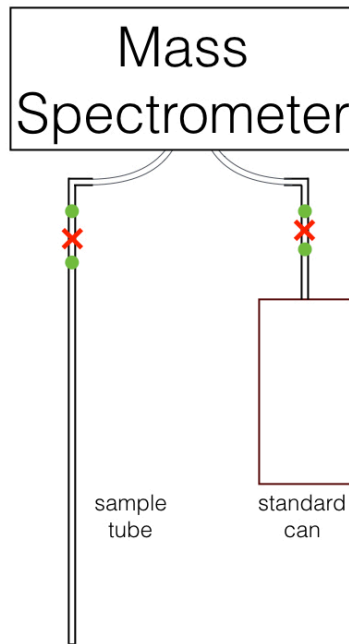


Figure 7: Schematic of how thermal fractionation test is setup on the mass spectrometer. Two temperature sensors (red x) are placed in between two valves (green dot) on both the sample tube and the standard can.

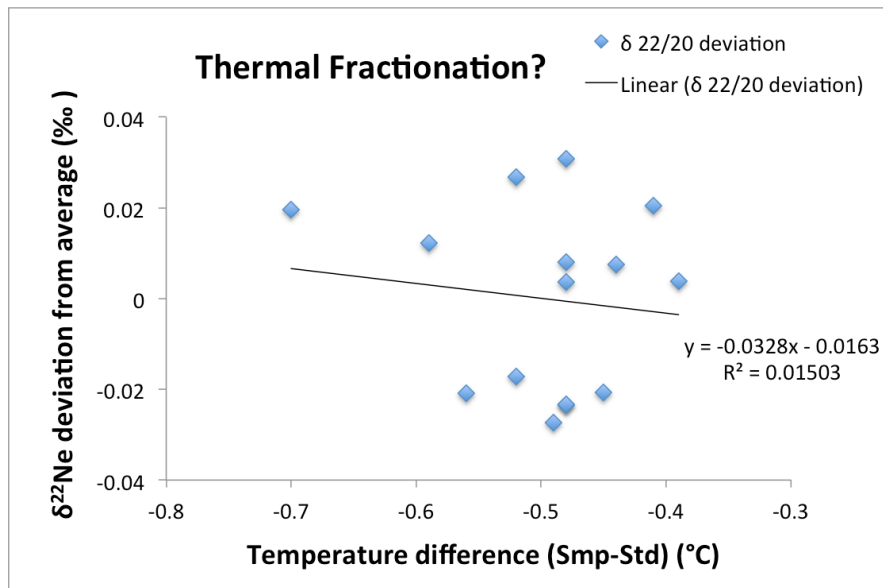


Figure 8: $\delta^{22}\text{Ne}$ deviation from the average due to temperature differences between sample and standard side. The low R-squared shows that there is no clear correlation between temperature and the observed $\delta^{22}\text{Ne}$ values.

3.5. Argon chemical-slope

Our neon extraction method removes >99.9% of the argon but is not perfect, so that argon cannot be completely removed. Therefore we measure the small remaining amount of argon in each sample, and then use the empirical sensitivity of $\delta^{22}\text{Ne}$ to argon (known as the argon chemical-slope) to make a precise correction for this largest of the interferences in our mass spectrometer measurements. The argon chemical-slope demonstrates how a varying amount of trace argon present in the sample will affect the $\delta^{22}\text{Ne}$ measurements on the mass spectrometer. In general, $\delta^{22}\text{Ne}$ increases/decreases nearly linearly with decreasing/increasing $^{40}\text{Ar}^{++}$ within a small range, so we can make a mathematical correction to the raw $\delta^{22}\text{Ne}$ measurements to get the true $\delta^{22}\text{Ne}$. Argon has a large $\delta^{22}\text{Ne}$ effect (section 1.3.1), so a chemical slope is required to make precise corrections.

The chemical slope is acquired from an experiment in which progressively larger amounts of pure argon are added to multiple aliquots of a pure, unfractionated neon standard, as is commonly done for other gases such as nitrogen or argon isotopes (Severinghaus et al., 2003). These aliquots are measured for neon isotopes and the argon/neon ratio. Because the true neon isotope ratio in all of these aliquots is the same, the only factor affecting the measured $\delta^{22}\text{Ne}$ is the interference from argon. The argon/neon ratio is measured using a “peak jumping” method, in which $^{40}\text{Ar}^+$ and $^{22}\text{Ne}^+$ beams are measured sequentially by changing the mass spectrometer magnet. Because $^{40}\text{Ar}^+$ and $^{22}\text{Ne}^+$ cannot be measured at the same time, and because the beams always decrease with time due to depletion of the sample gas, peak jumping of $^{40}\text{Ar}^+$ and $^{22}\text{Ne}^+$ is repeated twice in order to be able to make an interpolation in time to find their ratio as it would be if they were measured at the same time.

Our first attempt to remove argon from the sample only used mol-sieve once to trap argon. The single Ar removal chemical slope was found (Figure 9a; slope of the line formed by blue diamonds). Although we got an almost perfect correlation between amount of argon and observed $\delta^{22}\text{Ne}$, there was a substantial amount of argon left in the sample, so we decided to repeat the Ar removal step in the method. Using the mol-sieve twice was found to yield less interference by eliminating almost all Ar in the sample (Figure 9a aggregated red boxes). A zoom-in of the double-Ar-removal chemical slope is shown in Figure 12b. The *R*-squared of the double-Ar-removal chemical slope is not as good as the single-Ar-removal chemical slope, because the much smaller argon signal creates a lower signal-to-noise ratio and makes the relative measurement error larger, but this is acceptable.

In Figure 9a, the amount of argon apparently does not have a linear relationship with $\delta^{22}\text{Ne}$ when looking at a wider range. When more argon remains in the sample, the chemical slope is -14.93, and it becomes steeper at -15.37 when most of the argon is removed. This nonlinearity is an expected result of the fact that the interference is acting upon the denominator of the $^{22}\text{Ne}/^{20}\text{Ne}$ ratio, creating a hyperbola as more and more argon is added. For this first stage of method development, we ignore this hyperbolic relationship, and simply use the approximation that the slope is very nearly linear when >99.9% of the argon has been removed (an exact treatment of the hyperbolic relationship is given in Section 4.4.5). Therefore, two Ar removal steps are used for the method, and for now the argon chemical slope value of -15.37 is applied to give an approximately-corrected $\delta^{22}\text{Ne}$, which is closer to the true $\delta^{22}\text{Ne}$ value.

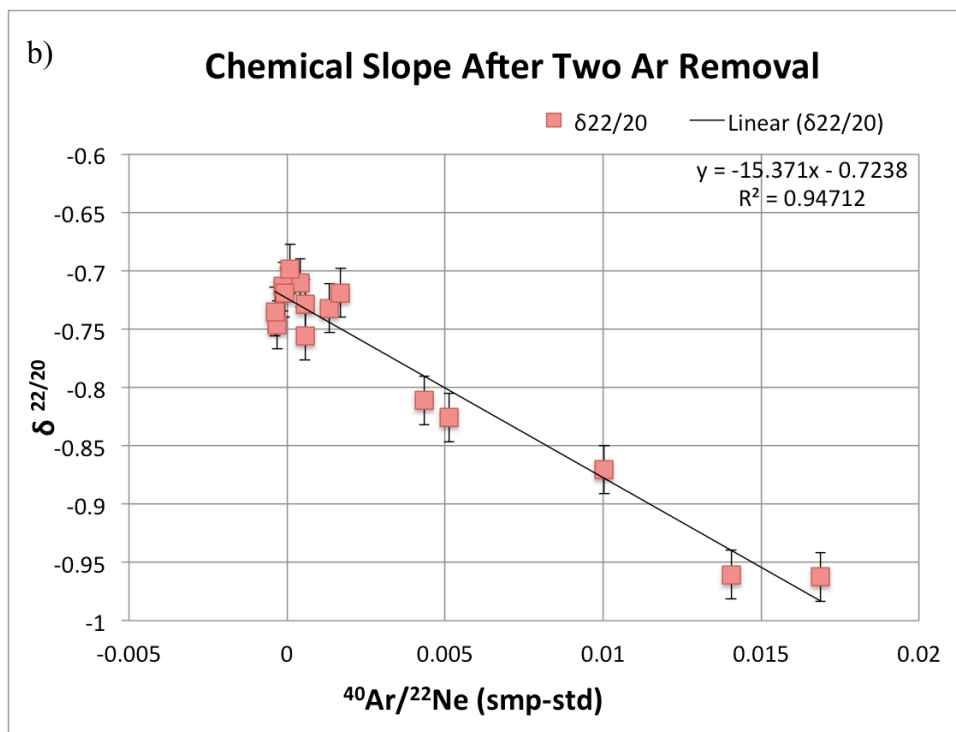
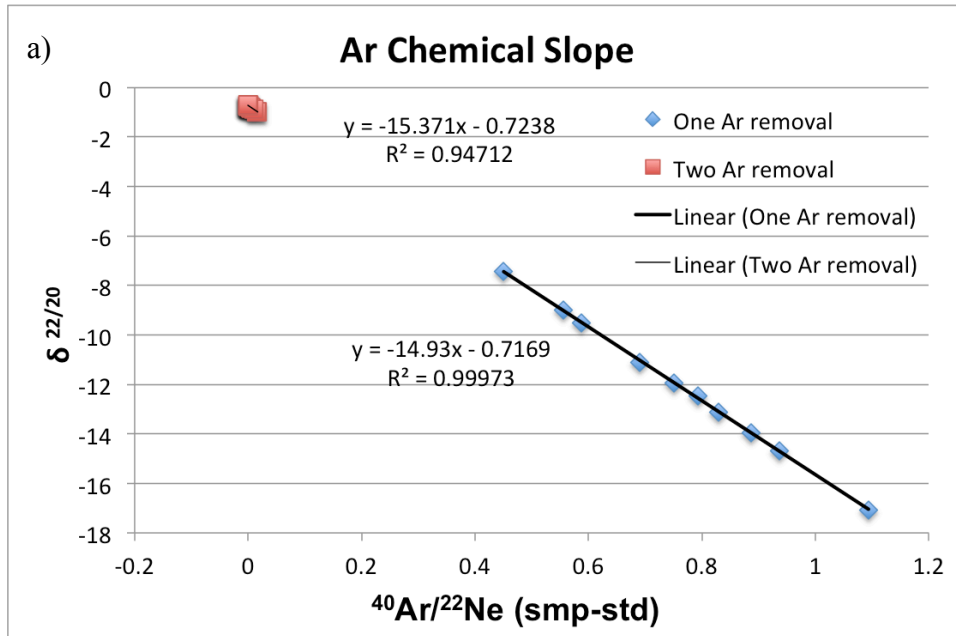


Figure 9: Comparison of Ar chemical slope generated from different procedures. a) Ar chemical slope for a single Ar removal step, and a double Ar removal. b) Zoom-in of Ar chemical slope for the double Ar removal.

3.6. Mathematical corrections

To get true neon isotope values, four corrections are applied to the raw data, and they are: (1) pressure imbalance correction, (2) doubly-charged ^{40}Ar ($^{40}\text{Ar}^{++}$) on singly-charged ^{20}Ne ($^{20}\text{Ne}^+$) isobaric interference correction, (3) doubly charged $^{44}\text{CO}_2$ ($^{44}\text{CO}_2^{++}$) on singly-charged ^{22}Ne ($^{22}\text{Ne}^+$) isobaric interference correction, and (4) ricochet N_2 ($^{28}\text{N}_2^+$) on ^{22}Ne ($^{22}\text{Ne}^+$) interference correction. In this first stage of method development, we applied the corrections in the order of first the pressure imbalance correction, followed by the Ar, CO_2 and N_2 corrections. The $^{40}\text{Ar}^{++}$ interference was corrected first because it affects the neon isotope measurements the most (in the 1‰ range). The corrections for $^{44}\text{CO}_2^{++}$ and $^{28}\text{N}_2^+$ interferences are quite small (in the 10^{-2} ‰ range), so approximating the interference effect was considered sufficient and the order of correction was not considered important.

3.6.1. Pressure imbalance correction

The intensity of the two neon beams on sample and standard sides are set to be the same at the beginning of each block of measurements, but the two sides become imbalanced over the course of a block (16 cycles), due to the fact that sample and standard never have exactly the same number of moles of input gas. The pressure imbalance correction follows Severinghaus et al. (2003). The pressure imbalance sensitivity (*PIS*) is calculated about once a week by:

$$PIS \equiv \frac{\delta_{\text{unbalanced}} - \delta_{\text{true}}}{\Delta_p} \quad (6)$$

$$\text{where } \Delta_p \equiv \left(\frac{V_{\text{sample}}}{V_{\text{standard}}} - 1 \right) \times 1000 \text{ ‰} \quad (7)$$

$\delta_{\text{unbalanced}}$ is measured by the mass spectrometer by deliberately adjusting the bellows of both the sample and the standard sides to obtain a 10% pressure difference at the start of a 16-cycle block.

δ_{true} is measured by the mass spectrometer with auto-balancing the pressure. The *PIS* so obtained is assumed to be constant over the course of about a week. Then the following equation gives the pressure imbalance correction that is routinely applied to each sample:

$$\delta_{PIS_corr} \equiv \delta_{measured} - (PIS) \Delta_p \quad (8)$$

3.6.2. Doubly-charged ^{40}Ar on singly-charged ^{20}Ne isobaric interference correction

The Ar interference is discussed in section 3.3.1, and the Ar chemical slope is explained in section 3.5. The correction is estimated by the following equation:

$$\delta^{22}\text{Ne}_{Ar_artifact} \approx \text{Chemical Slope} \times \left(\frac{^{40}\text{Ar}_{SA}^+}{^{22}\text{Ne}_{SA}^+} - \frac{^{40}\text{Ar}_{ST}^+}{^{22}\text{Ne}_{ST}^+} \right) \quad (9)$$

The quantity $\left(\frac{^{40}\text{Ar}_{SA}^+}{^{22}\text{Ne}_{SA}^+} - \frac{^{40}\text{Ar}_{ST}^+}{^{22}\text{Ne}_{ST}^+} \right)$ is known as the raw $^{40}\text{Ar}^+ / ^{22}\text{Ne}^+$ ratio difference between the sample and standard. The raw ratio difference is used because the sample is always being measured against a standard, and the $\delta^{22}\text{Ne}$ artifact from argon interference is caused by how much more argon is present in the sample than the standard. Also, measurements show that the standard cans do have a very small amount of argon, even though no argon is added when they are made. The typical raw ratio difference ranges from 0 to 0.02 (unitless), and sometimes the raw ratio difference can be negative, when the sample has less argon than the standard. The $\delta^{22}\text{Ne}$ argon interference correction is routinely calculated for each sample as:

$$\delta^{22}\text{Ne}_{Ar_corr} = \delta^{22}\text{Ne}_{PIS_corr} - \delta^{22}\text{Ne}_{Ar_artifact} \quad (10)$$

3.6.3. Doubly-charged $^{44}\text{CO}_2$ on singly-charged ^{22}Ne isobaric interference correction

During the pure neon and argon experiments, in principle there should not have been any source of CO_2 . However, some CO_2 always remains in the vacuum line and the mass spectrometer because CO_2 needs days to weeks to pump out once introduced. Instead of introducing CO_2 into the mass spectrometer to estimate the fraction (α_{CO_2}) of singly-charged $^{44}\text{CO}_2$ that becomes doubly-charged CO_2 , at this stage of method development we assumed that $\alpha_{\text{CO}_2} = 0.005$ based on prior measurements in Noble Gas Isotope Lab. The CO_2 interference is estimated to be:

$$\delta^{22}\text{Ne}_{\text{CO}_2\text{-artifact}} \approx \left(\frac{^{44}\text{CO}_2^+_{\text{SA}}}{^{22}\text{Ne}^+_{\text{SA}}} - \frac{^{44}\text{CO}_2^+_{\text{ST}}}{^{22}\text{Ne}^+_{\text{ST}}} \right) \times \alpha_{\text{CO}_2} \times 1000\% \quad (11)$$

where $\left(\frac{^{44}\text{CO}_2^+_{\text{SA}}}{^{22}\text{Ne}^+_{\text{SA}}} - \frac{^{44}\text{CO}_2^+_{\text{ST}}}{^{22}\text{Ne}^+_{\text{ST}}} \right)$ is the raw $^{44}\text{CO}_2^+ / ^{22}\text{Ne}^+$ ratio difference between the sample and standard. $^{44}\text{CO}_2^+ / ^{22}\text{Ne}^+$ is measured by peak jumping, and the reason for using the raw ratio difference of $^{44}\text{CO}_2^+ / ^{22}\text{Ne}^+$ is the same as for $^{40}\text{Ar}^+ / ^{22}\text{Ne}^+$. Then $\delta^{22}\text{Ne}$ with the carbon dioxide interference correction is routinely calculated for each sample as:

$$\delta^{22}\text{Ne}_{\text{CO}_2\text{-corr}} = \delta^{22}\text{Ne}_{\text{Ar-corr}} - \delta^{22}\text{Ne}_{\text{CO}_2\text{-artifact}} \quad (12)$$

3.6.4. Ricochet $^{28}\text{N}_2$ on ^{22}Ne interference correction

When nitrogen is ionized in the source of the mass spectrometer, a small number of nitrogen ions can be collected in the mass 22 Faraday cup due to a ricochet effect, where N_2 ions bounce off the internal walls of the mass spectrometer flight tube. Although the nitrogen interference is relatively small, it is not negligible. The fraction (α_{N_2}) of nitrogen ions that end

up in the mass 22 Faraday cup is estimated by introducing some pure nitrogen into the mass spectrometer:

$$\alpha_{N_2} = \frac{1}{\frac{^{28}N_2^+}{^{22}Ne^+}} = \frac{1}{\frac{57470919}{990}} = \frac{1}{130615} \quad (13)$$

where $^{22}Ne^+$ indicates the observed voltage in the mass 22 Faraday cup (even though it is not actually neon). The N_2 interference is estimated to be:

$$\delta^{22}Ne_{N_2_artifact} = \left(\frac{^{28}N_{2SA}^+}{^{22}Ne_{SA}^+} - \frac{^{28}N_{2ST}^+}{^{22}Ne_{ST}^+} \right) \times \alpha_{N_2} \times 1000\text{‰} \quad (14)$$

where $\left(\frac{^{28}N_{2SA}^+}{^{22}Ne_{SA}^+} - \frac{^{28}N_{2ST}^+}{^{22}Ne_{ST}^+} \right)$ is the raw $^{28}N_2^+/^{22}Ne^+$ ratio difference between the sample and standard. $^{28}N_2^+/^{22}Ne^+$ is measured by peak jumping and the reason for using the raw ratio difference of $^{28}N_2^+/^{22}Ne^+$ is the same as for $^{44}CO_2^+/^{22}Ne^+$ and $^{40}Ar^+/^{22}Ne^+$. Then $\delta^{22}Ne$ with the nitrogen interference correction is routinely calculated for each sample as:

$$\delta^{22}Ne_{N_2_corr} = \delta^{22}Ne_{CO_2_corr} - \delta^{22}Ne_{N_2_artifact} \quad (15)$$

3.7. Results after correction

The true $\delta^{22}Ne$ (Figure 10) is the value after making all the corrections (3.6.1-3.6.4). When we use the mol-sieve once, the external precision of 10 samples is 0.05 ‰ (red). The precision improved after we used the mol-sieve twice, where the external precision of 15 replicate samples is 0.02 ‰ (blue).

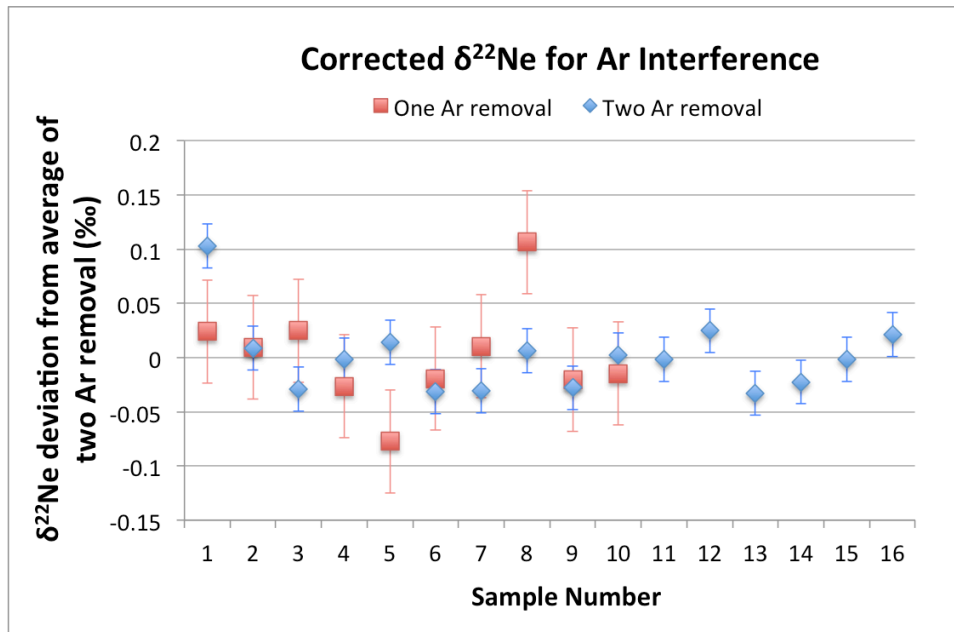


Figure 10: Corrected values for one and two Ar removal methods. Two Ar removal steps removes most of the argon and gives higher precision.

3.8. Discussion

At this first stage, the pure gases experiment, our developed method is able to measure neon isotopes at an external precision of less than 0.03 ‰. First, we found out that the mass spectrometer (MAT 253) we used can measure $\delta^{22}\text{Ne}$ in pure neon at an external precision of 0.01 ‰. Second, we showed that the 5Å mol-sieve is able to serve as the separator for argon and neon because the 5Å mol-sieve does not fractionate neon. Third, there is no thermal fractionation that we need to take into account. Fourth, we successfully removed argon by using the mol-sieve twice. Fifth, the precision of the developed method using pure gases, including gas handling on the extraction line, mass spectrometer capability, and the mathematical correction for interferences on $\delta^{22}\text{Ne}$ is 0.02 ‰. Next, we adapt the neon extraction method to air samples.

4. Method development – air extraction

After obtaining satisfactory external precision using pure gases, we moved on to the second phase of the method development, which is to make modifications to our method in order to extract neon from air and measure neon isotopes precisely. This is necessary because our sample from Greenland is air, and extracting neon from air samples can be more complicated than pure gases due to the existence of other gases. Hence, our goal is to find out whether we are able to get the same level of precision when we change from pure gases to air sample extraction.

We establish our air extraction method using the air from the modern atmosphere, which we call La Jolla air (LJA), because unlike the limited (and precious) Greenland firn air samples, there is no problem with sample availability. We also use LJA as our ultimate standard because it is homogenized on Earth within a year, and the neon isotopes are constant in the atmosphere within the relevant timescale of the last million years. The air extraction method was tested and modified during three different stages: (1) using dry LJA from a pressurized tank, (2) using dry LJA from the pier as the primary standard, (3) using Greenland air sampled at the surface of the firn (zero depth). In all cases these gases were compared against the working standard.

Dry La Jolla air was collected, pressurized to ~2000 psig, and modified by the Atmospheric Oxygen Research Group of Prof. Ralph Keeling at SIO. We use a tank of pressurized air for testing purposes for convenience, because we do not have to get air from the pier each time a sample is needed. However, the pressurized tank air is likely to be fractionated during the collection process or when the air is introduced to the extraction line, so it is not used as the primary standard.

4.1. How to remove most of the air?

A schematic of the changes made to the extraction line setup is shown in Figure 11. The air extraction method is similar to the pure gases extraction, except that we are introducing air into the vacuum line, instead of pure neon and argon. Pressurized air is fractionated when it is first introduced to the flask, so it is necessary to flush the air to waste in the room at a constant rate of 10 c.c./sec for 10 min. Then valves are closed in the order of the tank to the flask, so no fractionation occurs due to closing off a valve on a moving airflow. The collected aliquot of homogenized air has a pressure of 1 atm, which is convenient when we later transition to our ultimate method of standardization using La Jolla air collected from the pier at 1 atm.

We experimented with adding gettering to the method, which had been previously developed in the Scripps Noble Gas Isotope Lab to eliminate all gases except noble gases as a method of precise measurement of Ar 40/36 and Kr/Ar ratios in polar ice (Severinghaus et al. 2003). The getter “sheets” are an alloy of Zr and Al provided by the manufacturer (SAES). These sheets are placed in an oven, where the air undergoes the gettering process at 900°C after the oven is activated. Before turning off the oven, the gas is left in the same space for an additional 2 min at 300°C to absorb H₂ gas. Then the oven is turned off, and pressure is recorded with a capacitance manometer (MKS). The mixture of noble gases is then readied for removal of the argon in the adjacent glass tube that contains mol-sieve.

To get the same amount of neon that was previously used on the mass spectrometer with pure gases, we would need about 1 L STP of air. We tried to getter the air first and then separate argon and neon. However, after several experiments, we found that gettering was not practical for 1 L STP of air because the oven was not designed for large volume samples. The gettering process took more than 2.5 hours and the separation of argon and neon was not successful.

Rather than attempting to solve this problem, we decided to reduce the volume of air needed.

Several of our previous measurements showed that using a reduced amount of neon gives a similar level of precision. This means that only 160 ml of air is needed. Since we know the mol-sieve can trap nitrogen at 77K, we changed the method to use the mol-sieve and getter at the same time, to help reduce the amount of gas that needed to be gettered. Although the volume and method were adjusted, the total time needed was still more than 3 hours. The $\delta^{22}\text{Ne}$ measurements indicated the neon extraction method with gettering and molecular sieve was not successful.

Since gettering was not suitable for such an amount of air, we switched to using only mol-sieve because it can remove argon, carbon dioxide and nitrogen from the air sample, which is the main purpose of the method development. We increased the amount of mol sieve to two tubes (20 ml) and tried a 1 L air extraction again. Although I was not able to measure the two sample extractions I did, due to the lack of comparable standards at the time, it was apparent that mol-sieve alone is capable of trapping most of the air.

One problem we faced was that a noticeable amount of helium would typically show up on the convectron pressure gauge after the cryotransfer of neon to the 4 K dip-tube, and this residual gas can be confusing because it is difficult to determine whether or not there has been an incomplete transfer of neon. (More details are discussed in section 3.1) A test was done to find out what the convectron would show if normal atmospheric helium (5 ppm helium versus 18 ppm for neon) from the air sample is detected after transfer. Helium was added to a stainless steel can in an amount calculated based on what 1 L of air would have, and an aliquot of this helium was expanded into the line.. The convectron showed $2.1\text{e-}3$ torr, which is the

approximate residual seen after cryotransfers. We conclude that, if the residual is higher than 2.1×10^{-3} torr, then there is a high possibility of a neon residual and an incomplete transfer.

Pressurized dry LJA aliquots are not adequate to be the primary standard gas, as mentioned earlier. At this point it was decided to skip further use of pressurized air and go directly to LJA collected in a non-fractionating manner, as this is the ultimate primary standard that is needed. Therefore we began to use LJA collected from the pier.

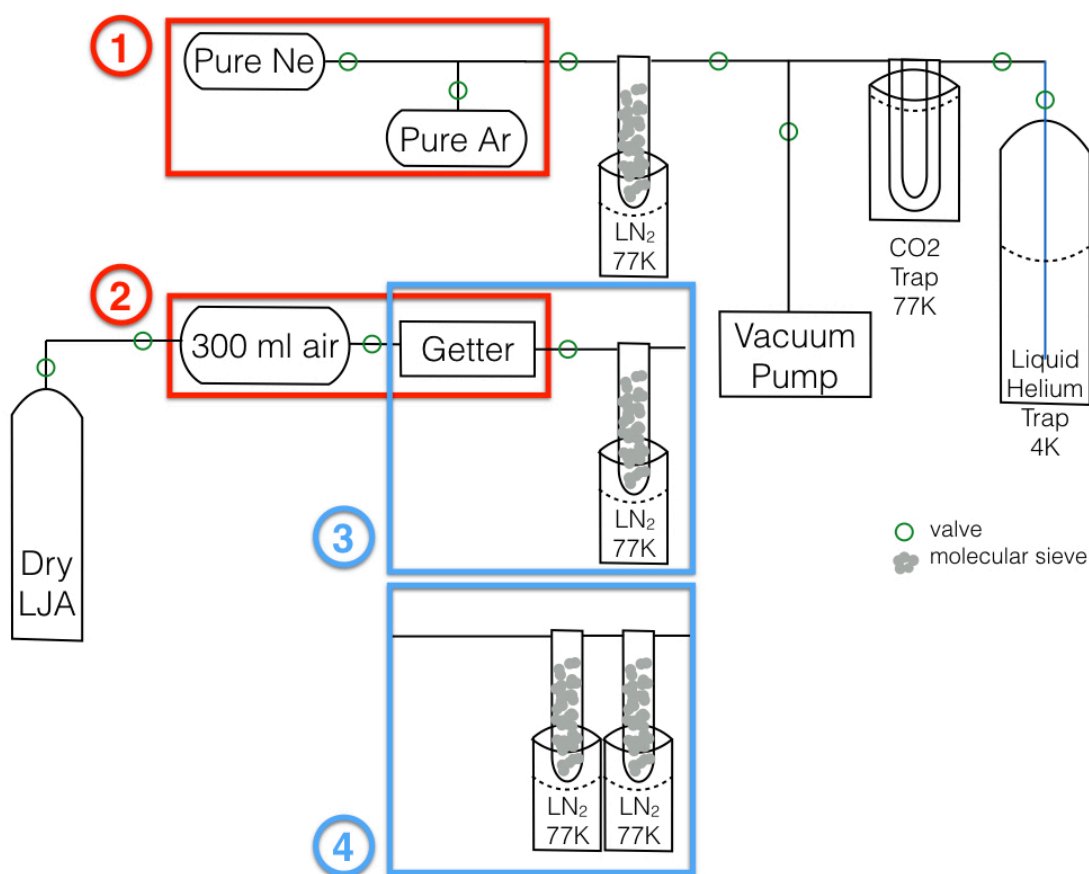


Figure 11: Schematic of the extraction line modification throughout the method development with a pressurized cylinder of LJA. First, we added getting to the neon extraction method (red box 2 replaced red box 1). Then, we switched to using mol-sieve only when we found out that getting is not necessary (blue box 4 replaced blue box 3).

4.1.1. Does rapid air trapping fractionate neon isotopes?

Through method development, we found that 5Å mol-sieve in LN₂ temperature (77K) can not only trap argon, but also trap other abundant gases in the atmosphere, such as nitrogen, oxygen, and carbon dioxide. No quantitative measurements were done on how much 5Å mol-sieve is needed for a specific amount of each gas. However, we found that two full 10 ml quartz tubes of mol-sieve are enough for about 1L of air, which is more than enough for air aliquot extraction. Any remaining gases after the mol-sieve treatment should not affect neon measurements substantially because the three main interferences are doubly-charged ⁴⁰Ar on singly-charged ²⁰Ne, doubly-charged ⁴⁴CO₂ on singly-charged ²²Ne, and ricochet ²⁸N₂ on ²²Ne.

An experiment was done with only nitrogen and neon to find out whether some neon gets trapped by the mass action of the rapidly moving N₂ and fractionated when the mol-sieve in LN₂ is used to remove most of the gases quickly from an aliquot of air (Figure 12). Nitrogen was chosen because it is 78% of the volume in air. If neon does not get fractionated when mol-sieving nitrogen, we assume that removing the other abundant gas oxygen, which is 20.95% of the volume, will neither cause noticeable fractionation.

Commercially made ultra-high purity nitrogen was cleaned with mol-sieve first to make sure that all of the neon collected in the dip tube only comes from our standard can of commercially made pure neon. The average $\delta^{22}\text{Ne}$ of the pure neon standard without adding any nitrogen was 4.21 ‰ with a standard deviation of 0.049 ‰. The average $\delta^{22}\text{Ne}$ of pure neon when adding cleaned ultra-high purity nitrogen that is rapidly removed by mol-sieve in LN₂ was 4.22 ‰, with a standard deviation of 0.031 ‰. The average of the two results are very close and within one standard deviation, so we conclude that the process of trapping nitrogen rapidly does not fractionate neon isotopes.

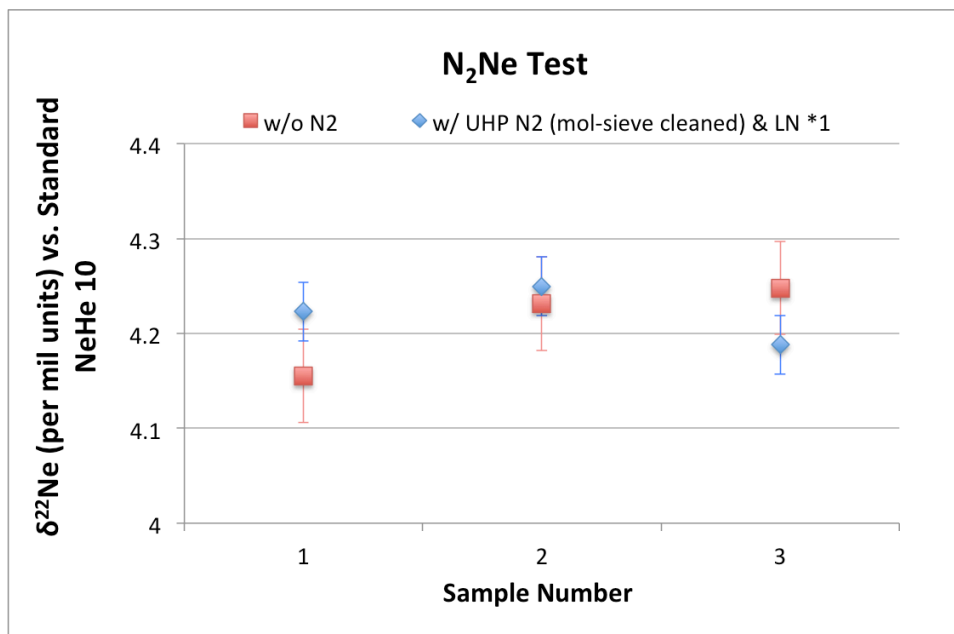


Figure 12: Comparing the neon isotope measurements of the pure neon and the neon after mol-sieving nitrogen. Trapping nitrogen with mol-sieve does not cause measurable neon fractionation.

4.2. La Jolla air as the standard

The first attempt at extracting neon from LJA began with expanding it from a 2L flask to the 1L-aliquot flask. The best external precision we were able to get was 0.13 ‰, after adjusting the transfer time (for comparison, the external precision for pure gas separation is 0.02 ‰). Processing a large amount of air increases the risk of failing to completely remove undesired gases, potentially lowering the external precision. Therefore, we decided instead to switch to a smaller volume, a 160 ml-aliquot. We knew that the amount of neon from 160 ml air is sufficient to get the desired precision, because measurements of standard cans containing a similar amount of neon gave the desired precision.

Here, we first present the values of $\delta^{22}\text{Ne}$ of LJA versus our arbitrary working standard (Figure 13). With unpressurized LJA, we did three sets of experiments with slightly different

methods. The following is the one that we chose to use, and further explanation is given in Section 4.2.1. The average is -0.035 ‰ and the external precision is 0.06 ‰ . Although this does not meet the requirement of 0.03 ‰ , this seemed to be the best result we could get at this stage of development. The next stage was to use the same extraction method to extract Greenland firn air.

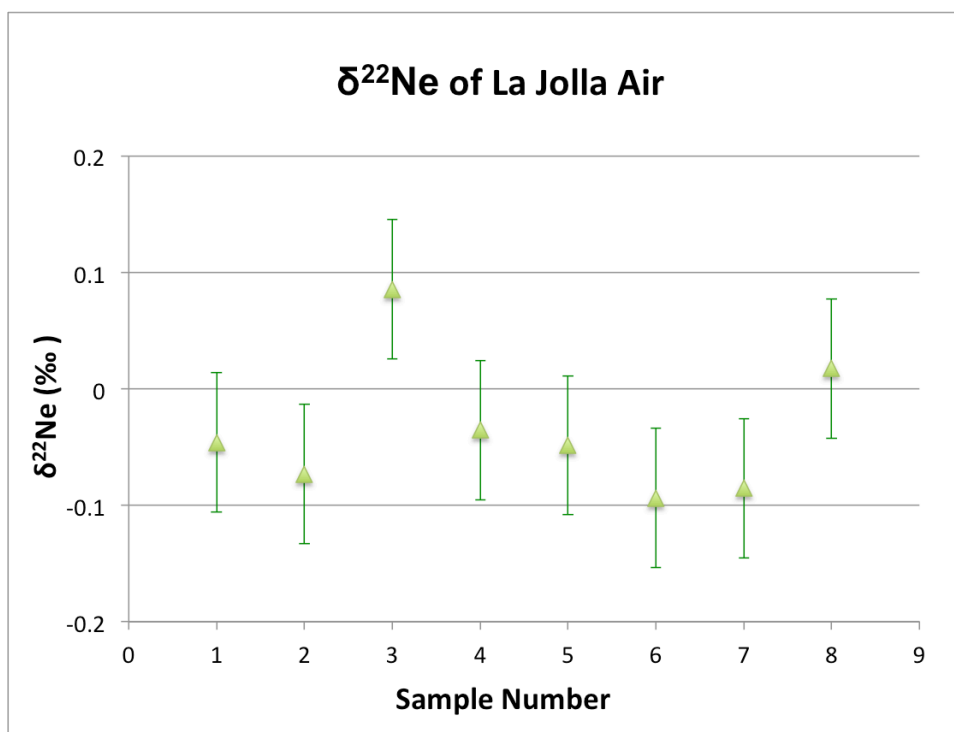


Figure 13: Corrected $\delta^{22}\text{Ne}$ of LJA. The average is -0.035 ‰ and the external precision is 0.06 ‰ .

4.2.1. Timing of mol-sieve in liquid nitrogen

This is the first time the Scripps Noble Gas Isotope Lab has developed a neon extraction method using 5 \AA mol-sieve, so the amount of time necessary to remove undesired gases is unknown. From prior experience when first developing the separation of pure gases with the

mol-sieve, we know that argon can be removed within 10 minutes, and we needed about 25 minutes for 1 L of air. Therefore, we hypothesized that the mol-sieve time for 160 ml air will be between 10 and 25 minutes. To find the optimal mol-sieve time, three sets of eight experiments were done with the same extraction procedure, except that the mol-sieve time was changed during the first Ar removal. Three different mol-sieve timings generated differing results and Ar chemical slopes (Figure 14). Most of the Ar was removed when leaving the mol-sieve in LN₂ for 20 and 15 minutes; slightly more of the Ar remained in the sample when the mol-sieve step was done for 10 minutes.

Although it is desirable to remove as much Ar as possible, to minimize the interference, in the end we chose to use only 10 minutes of mol-sieving. The reason is that both the 20 and 15 minute treatments generated anomalously low Ar chemical slopes compared to what we have been seeing from the pure gas experiments. Also, both *R*-squared values show that the slopes are not as linear as the 10 minute slope. Furthermore, the 10 minute mol-sieving aliquots have the best external precision of 0.06 ‰ after all mathematical corrections (Figure 15).

After we decided on the timing of mol-sieve in LN₂, the neon extraction method for air samples was developed. The procedure is summarized below: first, an aliquot of air is introduced into the vacuum line from a 2L flask; second, the air is exposed to clean mol-sieve in LN₂ (77K) to trap unwanted gases, such as nitrogen, oxygen and argon, for 10 minutes, and then the remaining gases (mostly neon) are collected in a dip-tube in LHe (4K); then this tube is placed on the vacuum line again for the second removal process, which is another 10 minutes of mol-sieve in LN₂, and the remaining gases (mostly neon) are collected in a double-valve dip tube; next, helium is added in between the double valve; lastly, we allow the helium and neon to homogenize in the tube for at least an hour before measuring it with the mass spectrometer.

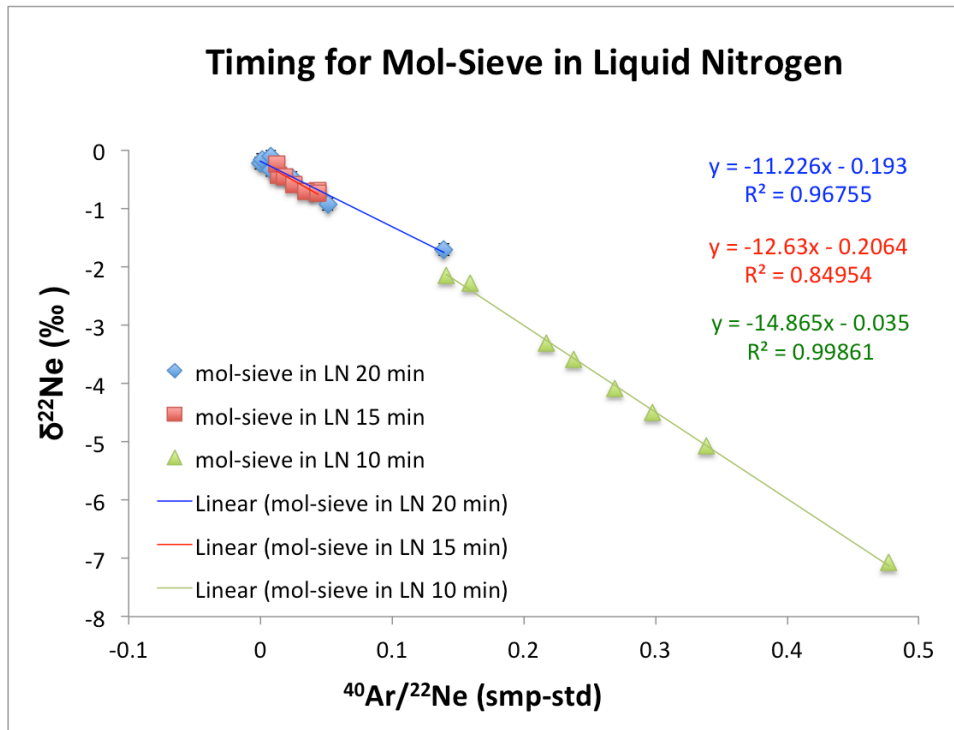


Figure 14: Ar chem-slope for different separation timings. 10 minute mol-sieving gives the best slope for precise Ar interference correction.

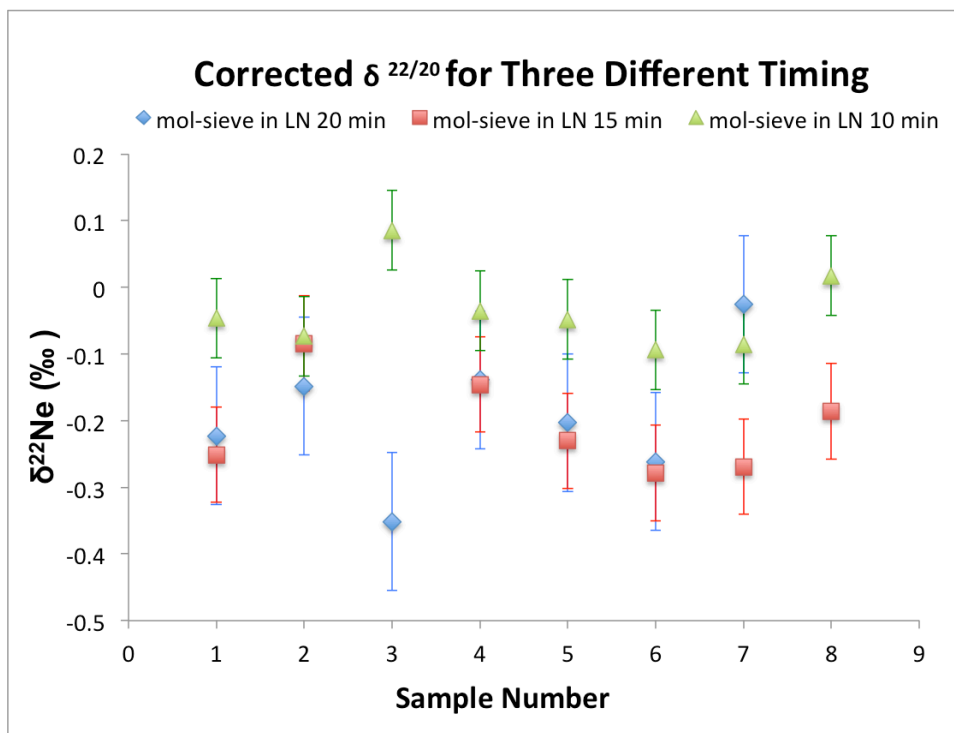


Figure 15: Corrected $\delta^{22}\text{Ne}$ for different timings with their corresponding Ar chem-slopes. The external precision is 0.103 per mil for 20 min; 0.072 per mil for 15 min; and 0.06 per mil for 10 min.

4.3. Surface Greenland air

The configuration of the vacuum line was slightly changed because the firn air sampling in Greenland did not remove water vapor, so it is necessary to trap out the water vapor. A water trap was added in between the Essex tank and mol-sieve, to prevent water molecules from saturating the mol-sieve and reducing the efficiency of undesired gas removal (Figure 16). The Surface Greenland air (SGA) extraction method is slightly modified from that of LJA. A sample of SGA is introduced by quickly opening and closing the 4H valve on the Essex tank, followed by placing LN₂ on the water trap for 5 minutes to freeze most of the water vapor. The rest of the extraction procedure is the same as previously described.

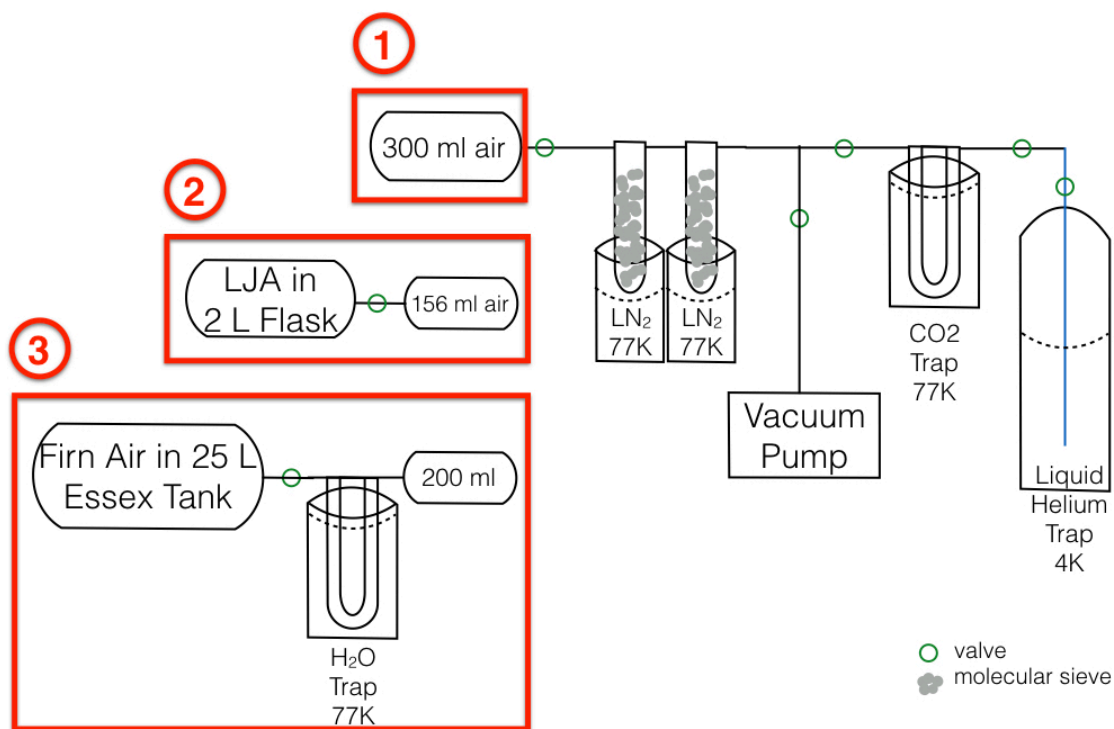


Figure 16: Schematic of method development using LJA from the pier and similar setup for Greenland firn air. Dry LJA from pressurized cylinder is replaced by LJA from the pier (red box 2 replaced red box 1). One flask of LJA air is measured several times by expanding it to a smaller volume. When we switched to Greenland firn air samples, a water trap was added because the field collection process did not eliminate water vapor (red box 3 replaced red box 2).

The SGA measurements began with the surface tank, at a depth of 0 m, because $\delta^{22}\text{Ne}$ at the surface should be isotopically the same as LJA since air is well mixed in the atmosphere. Air from deeper having any deviation from the SGA surface measurements will be interpreted as evidence of natural fractionation. A total of 10 SGA extractions and measurements were made, but none of them were within error of the LJA measurements (Figure 17).

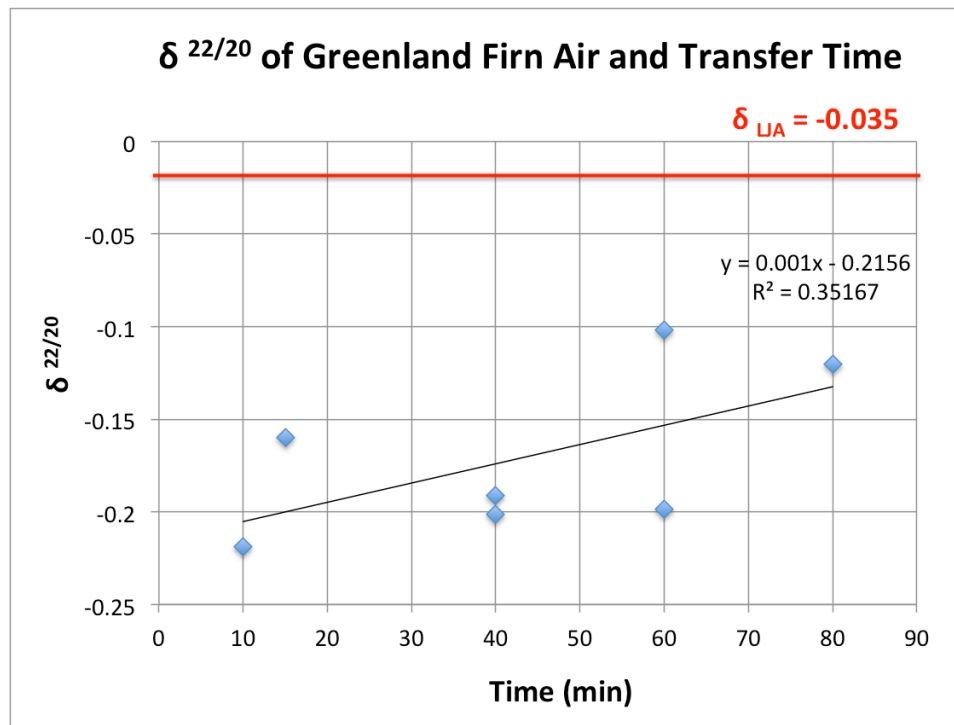


Figure 17: Delta values of the surface firn air plotted vs. transfer time.

4.4. Discussion: Why SGA≠LJA?

4.4.1. Incomplete transfer?

In principle, incomplete transfers could become a problem if a large volume is added onto the extraction line with the transfer time remaining the same. Insufficient transfer time can possibly leave some heavily-fractionated gas behind, not collecting it into the dip-tube. One

possible reason for an incomplete transfer (at 10 minutes) might be the vacuum line configuration change. To test this hypothesis we did several extractions at longer transfer times: 40 min, 60 min and 80 min (Figure 17). Although the results show a very weak trend of $\delta^{22}\text{Ne}$ with transfer time, the scatter is large and in any case it is impractical to increase the transfer time to 100 minutes or more. Hence, the problem remained unsolved.

A second test was done of the larger-volume hypothesis. First, pure neon was added to the vacuum line and transferred from the small volume containing the mol-sieve only, which is the same volume used for the separation of a pure gas mixture, so we know that a 10 minute transfer is sufficient. Second, neon was transferred from the combined volume with mol-sieve and the added volume that connects the firm air Essex tank, for 10 minutes. The $\delta^{22}\text{Ne}$ for the smaller volume was 28.149 ‰, and the larger volume was 28.138 ‰. They are not significantly different. With this result, we confirmed that 10 minutes is enough to collect all of the neon even when the volume has doubled, so we reject the hypothesis.

4.4.2. Problem caused by the additional water trap?

We speculate that something unknown could be happening with adding a water trap before the mol-sieve because this part was not present when we extracted LJA, so we tried one extraction without putting the water trap in LN_2 and one extraction changing the LN_2 (77K) to ethanol (193K). Both transferred for 10 minutes, and the results fall within the range of the 10-minute LJA transfer shown in Figure 17. These two experiments also show that neon is not being blocked by water vapor frozen in the water trap.

4.4.3. Leak in from room air neon on the vacuum line or mass spectrometer?

Both the extraction lines and the mass spectrometer are under high vacuum, so there is a potential detectable neon leak in from the room. For the vacuum lines, a “leak test” has to be passed before any sample extraction process is begun. A “leak test” is done by closing the valve to the turbo pump for 30 seconds and ensuring that the pressure in the vacuum line does not increase by more than 1×10^{-4} torr on the convectron gauge. Besides the leak test, another test was done to confirm that there is no neon leaking in from the room while transferring, by varying the transfer time. First, no gas was added to the vacuum line, and anything that was leaking into the vacuum line was collected into a dip-tube at 4K for 3 min (Ne Leak Test 4). Second, the same method was performed, except gas was collected for 60 min (Ne Leak Test 5). Figure 18 shows the zoom in of two magnetic field versus intensity scans of mass 20 and 22. These two scans have the same intensity so there should not have been any detectable leak during gas collecting. We did not add any neon to the vacuum line, so the detected mass 20 and 22 were more likely due to doubly-charged ^{40}Ar and $^{44}\text{CO}_2$, not singly-charged ^{20}Ne and ^{22}Ne .

For the mass spectrometer, a test was done by changing the equilibration time on the sample side to find out whether neon might leak in from the room through the o-ring (Figure 19). One aliquot of gas was introduced into the bellows on both sample and standard sides of the mass spectrometer. In the first set of experiments, both sides were homogenized for 5 minutes (5 min v. 5 min). In the second set, the sample side was introduced to the bellows first for 50 minutes and then for another 5 minutes while the standard side was introduced (55 min v. 5 min). Both were repeated three times. One of the 5 min v. 5 min results is different from the rest due to argon interference, because a higher raw ratio $^{40}\text{Ar}/^{22}\text{Ne}$ measurement on the sample side is observed, which produced a more negative $\delta^{22}\text{Ne}$. This particular one was discarded because the

precise mathematical interference correction has not yet been developed. The average $\delta^{22}\text{Ne}$ of the two 5 min v. 5 min is 0.017 ‰ and the standard deviation is 0.007 ‰. The average $\delta^{22}\text{Ne}$ of the three 55 min v. 5 min is 0.032 ‰ and the standard deviation is 0.018 ‰. Although the external precision of 55 min v. 5 min is larger than 5 min v. 5 min, it is within the required precision, 0.03 ‰. The three 55 min v. 5 min $\delta^{22}\text{Ne}$ results agree with each other, and the two 5 min v. 5 min. $\delta^{22}\text{Ne}$ fall within the possible error of the 55 min v. 5 min. Therefore, the o-ring does not cause a noticeable room air leak even with a long equilibration time.

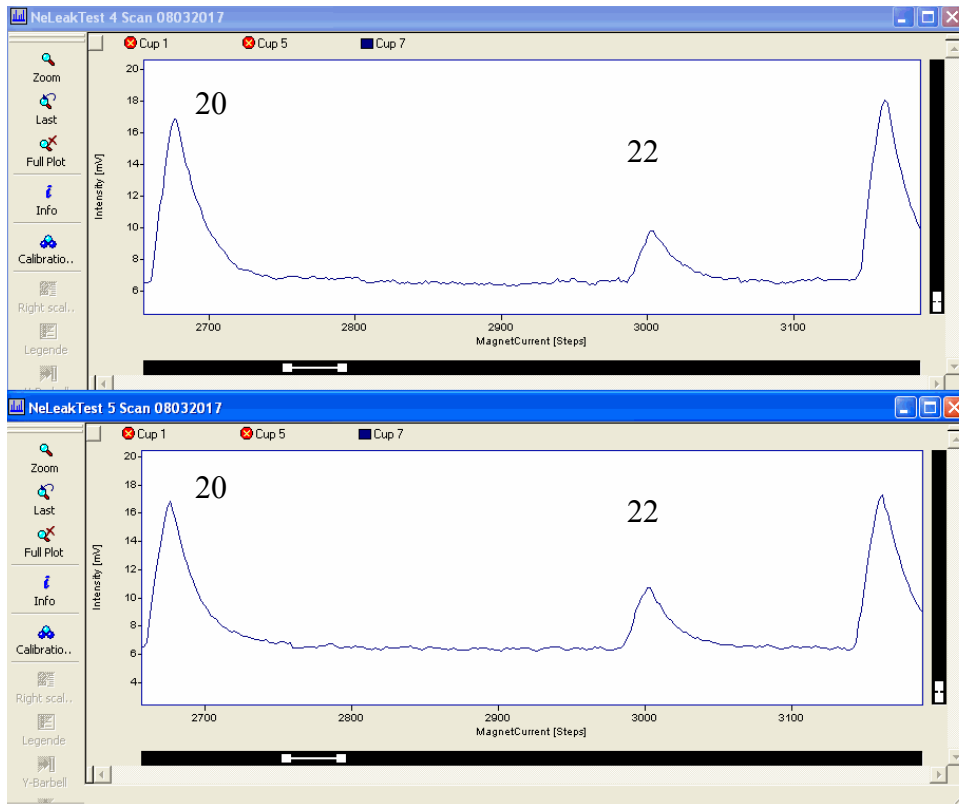


Figure 18: Zoom-in of both tests, Ne Leak Test 4 and 5. This magnetic field v. intensity scan only shows mass 20 to mass 22. There is no detectable room neon leaking into the vacuum lines while transferring.

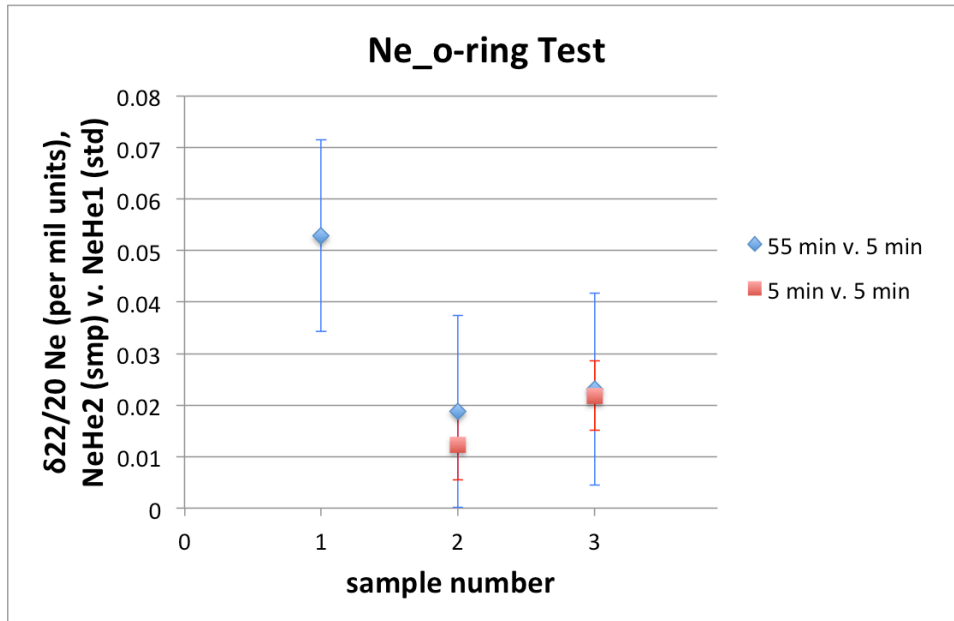


Figure 19: Comparison of $\delta^{22}\text{Ne}$ with different equilibration times on sample side. There is no detectable effect of room neon leaking in through o-ring while equilibrating gases in the bellows of the mass spectrometer.

4.4.4. Is there neon contamination from the ultra-pure helium?

The purity of our helium gas was verified by doing a magnetic v. intensity scan of an aliquot of helium from the commercial helium tank (Figure 20). The amount of ions (in voltages) is shown in Table 2. In Figure 20, the signals are from the $1\text{e}12 \Omega$ resistor Faraday cup. The left column is the scan from the helium tank, and right column is the scan of the machine background. Small amounts of mass 20 and 22 ions are detected, but they might not be true ^{20}Ne and ^{22}Ne ions, because some ^{40}Ar and $^{44}\text{CO}_2$ are measured. The amount of ^{40}Ar is acceptable. There seems to be some amount of $^{44}\text{CO}_2$, but it is more likely to be from the mass spectrometer itself because $^{44}\text{CO}_2$ is known to be “sticky” and takes a long period of time to remove. There are also nitrogen ions collected, but their source is not clear. However, the ricochet nitrogen interference is relatively small, so this amount should be acceptable. There are no influential amounts of neon, nitrogen, argon, nor carbon dioxide present, so using commercially made

helium in the method will not affect neon isotope values. In addition, if the presence of these gases happened to have some affect, it would likely be the same on both the sample and the standard side, which means the $\delta^{22}\text{Ne}$ will not be affected.

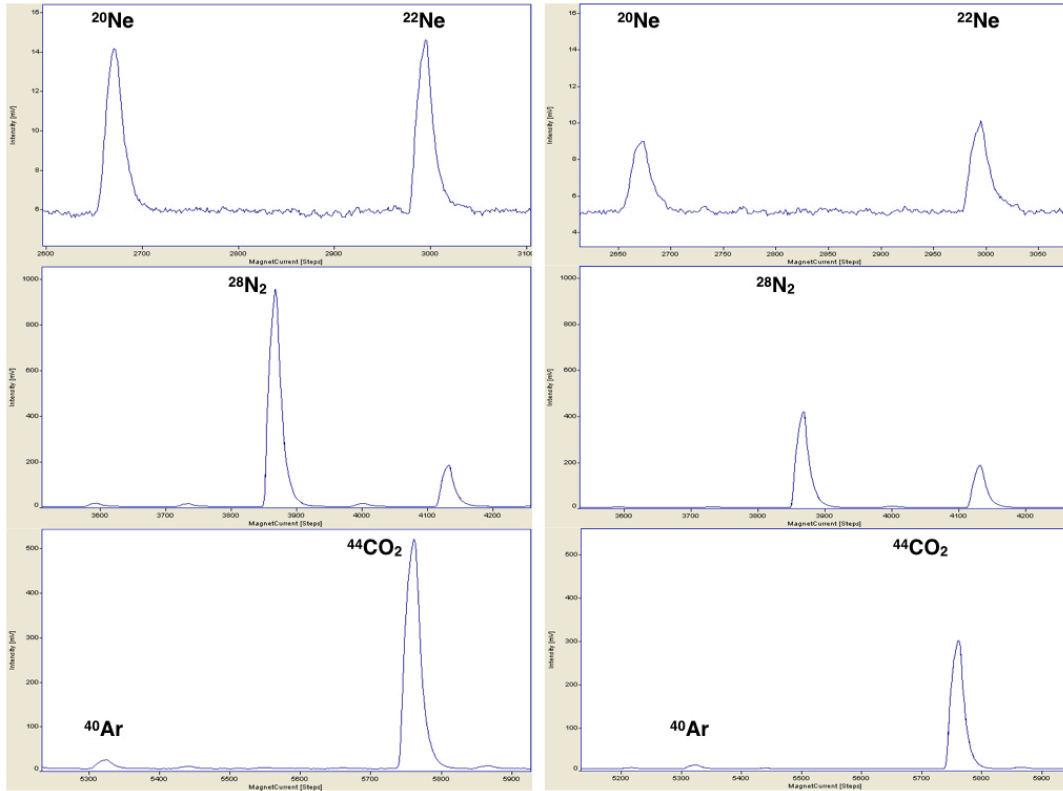


Figure 20: The magnetic v. intensity scan of the commercial high purity helium gas tank. The ultra-purity helium gas tank is pure enough that adding helium to the samples will not affect neon isotope measurements.

Table 2: Collected ions of neon isotopes, nitrogen, argon, and carbon dioxide in voltage from the magnetic v. intensity scan of Figure 20. This table provides quantitative evidence to prove the ultra-purity helium gas is sufficiently clean to use.

	Helium gas (mV)	Background (mV)	Differences (mV)
Ne-20	14.16	8.85	5.31
Ne-22	14.59	10.1	4.49
N ₂ -28	957.2	419.96	537.24
Ar-40	25.76	14.34	11.42
CO ₂ -44	520.23	301.21	219.02

4.4.5. Insufficient mathematical corrections?

It is puzzling that we could not find out why the surface SGA result differs from LJA. The examinations above showed that the problem is not from the extraction process on the vacuum line, so we also did inspections on the mass spectrometer. Not all of the details are included in this thesis, but we concluded that no leaks were found and no contamination exists within the mass spectrometer. In this circumstance, one remote possibility to explain the problem could be inadequate mathematical correction for isobaric and ricochet interference.

We started with checking whether we have the correct values of the constants, such as the fraction of $^{40}\text{Ar}^+$ and $^{44}\text{CO}_2^+$ that becomes doubly charged, and the fraction of N_2^+ that ricochets. In principle, these constants should not change dramatically unless the ion source of the mass spectrometer has changed. The fraction of $^{40}\text{Ar}^{++}$ is not directly measured on the mass spectrometer, but the correction for this interference is determined by the argon chemical slope, which did not change.

To probe the fraction of $^{44}\text{CO}_2^{++}$, we put an aliquot of pure CO_2 into the mass spectrometer, and discovered that the fraction of $^{44}\text{CO}_2^{++}$ is not 0.005, but 0.013. The old value was measured on a different mass spectrometer in the past. We did not verify this constant previously, because we did not expect it to be very different. The fraction of N_2^+ that gets collected in the mass 22 Faraday cup also changed, from $1/130615 \approx 7.6\text{e-}6$ to $1/105700 \approx 9.5\text{e-}6$, a small increase. In view of these increases, we decided to use a more precise mathematical correction for the interferences. With careful derivations, we realized that the following assumptions were not adequate: (1) the raw peak jumping measurements of 40/22, 44/22, and 28/22 by the mass spectrometer are the true ratios; and (2) the order in which the interference corrections are made does not affect the result significantly.

In place of the approximate mathematical corrections that had been used previously, we developed exact mathematical corrections for all three interferences. We also discovered the following: (1) Instead of using δ , we needed to make all of the interference corrections with q , which is $\delta/1000 + 1$, to make the calculations exact and to adequately treat the hyperbolic nature of the argon interference; and (2) The fraction of $^{44}\text{CO}_2$ ions that are doubly-charged can vary from time to time, so it is necessary to measure this fraction before starting a series of analyses. (3) The neon measurement sequence on the mass spectrometer has to be altered because the raw ratio of 44/22 appears to be different after each block of measurements. Therefore, a peak jumping measurement of mass 44/22 is added after each block to make a more precise correction for the doubly-charged $^{44}\text{CO}_2$ interference. (4) The correction order is important because the magnitude for each correction varies widely, and errors can be increased if large corrections are done first using uncorrected observations. The order has to be from the smallest magnitude correction to the largest, which is from N_2 , to CO_2 , to Ar. It is important to make the Ar correction last, because it critically depends on an accurate observation of the $^{40}\text{Ar}/^{22}\text{Ne}$ ratio, which is affected by $^{44}\text{CO}_2^{++}$ interference in the denominator. This way, the observed 40/22 ratio best corresponds to the true amount of Ar remaining in the sample.

Here, we will present how the change of correction method affected the magnitude and neon isotope values for one typical sample (Figure 21) and a set of samples (Figure 22). The new equations will be shown in section 5.2 and the derivation of the more precise mathematical corrections is included in the Appendix. Figure 21 shows that the correction always begins with the pressure imbalance correction, as before. The combined effect of the improved correction method and order changes the $\delta^{22}\text{Ne}$ value about 0.07 ‰ for one particular sample. For 10

samples, the average is different by 0.05 ‰ (Figure 21). In addition, the external precision improved from 0.122 to 0.023 ‰, which meets the requirement of being 0.03 ‰ or less.

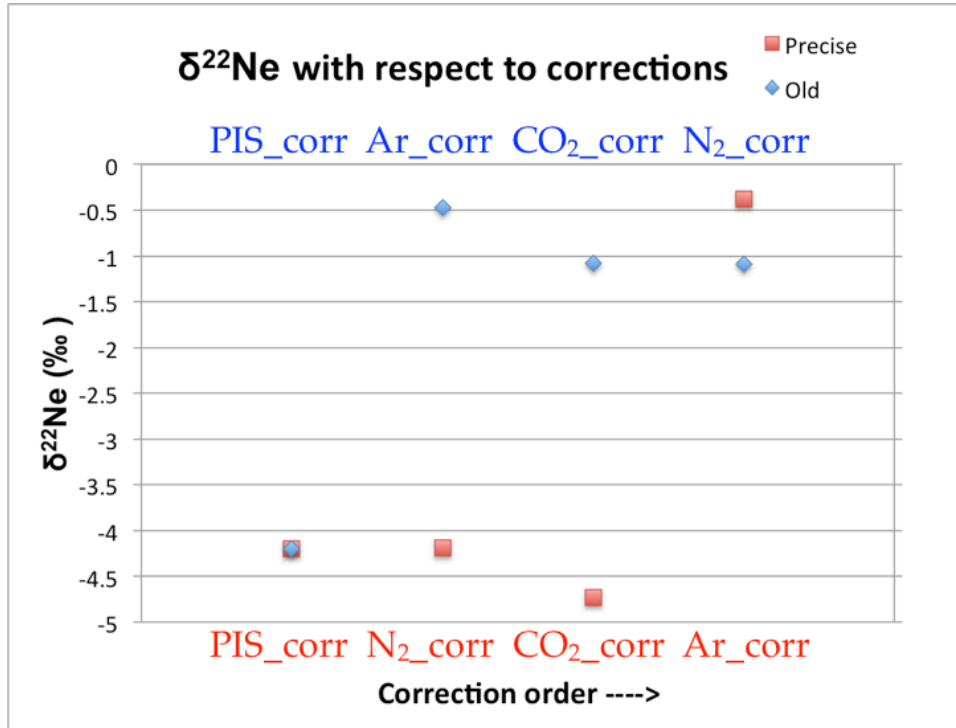


Figure 21: The combined effect of modified correction order and calculation. Both calculations begin with PIS corrected δ²²Ne from the left but differ in order for argon, carbon dioxide and nitrogen interferences. The old corrections give δ²²Ne heavier than the modified ones.

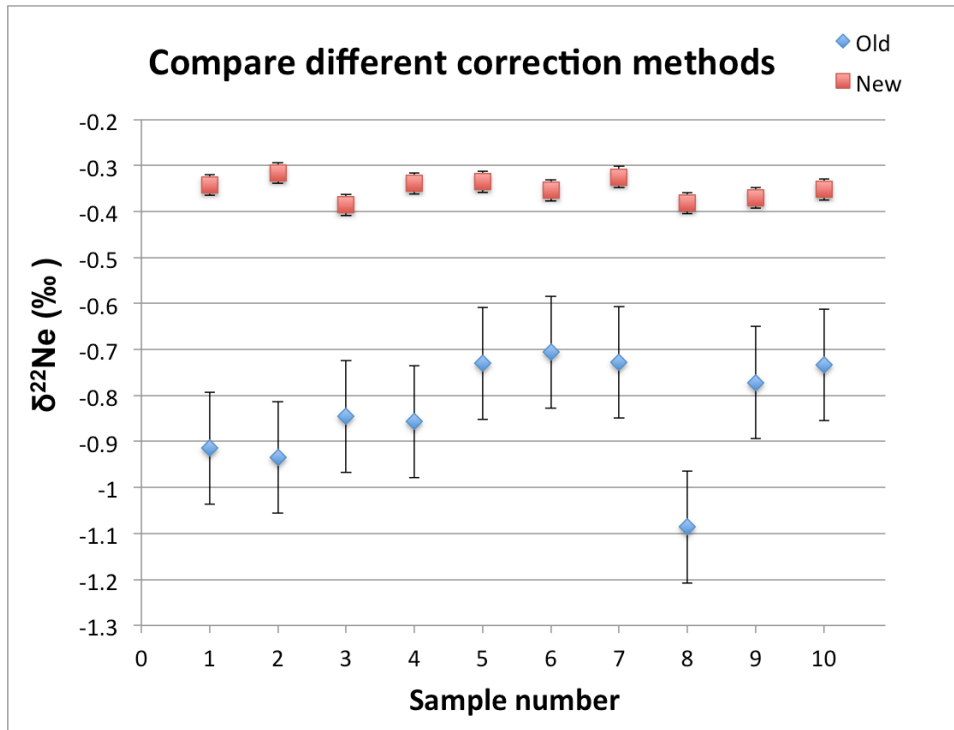


Figure 22: Comparison of how two different correction methods affect $\delta^{22}\text{Ne}$. For 10 replicates, the older method gives average of -0.83‰ and precision of 0.122‰, and the modified calculation method gives average of -0.35‰ and precision of 0.023‰.

5. Method development – second attempt of air extraction

After carefully examining all possibilities, we did not find the problem that causes SGA to be so different from LJA. Inadequate interference correction was probably part of the reason why the external precision was not good enough, because they apply to both LJA and SGA. We did what we could, and wanted to try extracting LJA again to see if the SGA problem had gone after making some adjustment on the extraction line, the measuring method on the mass spectrometer, and the interference corrections.

5.1. Adjustments for the second attempt

We decided to make an adjustment on the extracting LJA, which is to add a water trap even though this is not necessary for LJA. This will make everything the same on the extraction line for both LJA and SGA. The measuring sequence was changed by adding measurement of 44/22 after each of the 16-cycle neon isotope ratio measurement blocks, and repeats this three times. Then each of the $^{44}\text{CO}_2^{++}$ interference corrections will be applied to the 16-cycle neon isotope ratio measurement block accordingly. We also added background measurement for neon-22 and argon-40, so we get a more precise measurement by subtracting what was in the mass spectrometer already.

Most of the required constants for the interference corrections were changed because at this point the mass spectrometer was baked and the source was re-focused. The new Ar chem-slope is 0.0144, which was acquired by adding various amounts of Ar (Figure 23), and the slope was found to remain the same for all ranges as long as the source did not change. The new α_{CO_2} measured is 0.019, and we assume α_{N_2} did not change because the ricochet effect is not dependent on the focusing of the source.

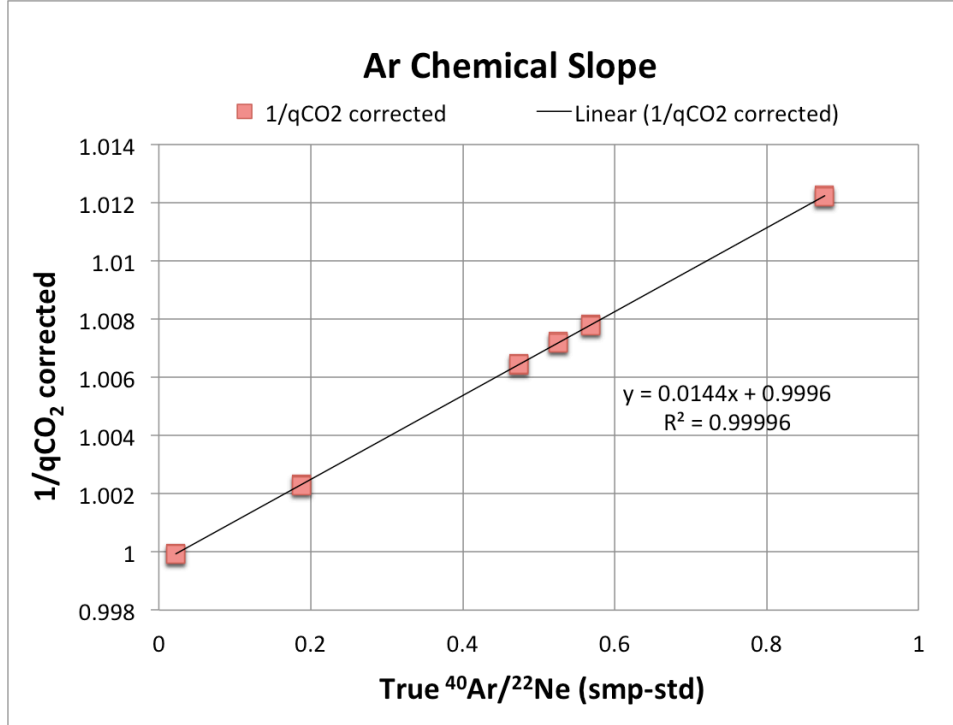


Figure 23: Ar chem-slope for exact corrections. The slope is 0.0144. The hyperbolic nature of Ar interference is treated by taking the reciprocal of the CO_2 -corrected $q_{22/20}$.

5.2. Exact mathematical corrections

5.2.1. Pressure imbalance correction

The very first correction for raw $\delta^{22}\text{Ne}$ is the pressure imbalance correction (Severinghaus et al., 2003) and the math remains the same (eq. 8-10). Next is the ricochet interference correction for $^{28}\text{N}_2/^{22}\text{Ne}$, which begins with PIS-corrected δ and converts it back to q , as represented by the following:

$$q_{\text{PIS}_{\text{corr}}} = \frac{\left(\frac{22}{20}\right)_{\text{SA}}}{\left(\frac{22}{20}\right)_{\text{ST}}} = \frac{\left(\frac{^{22}\text{Ne}^+ + \alpha_{\text{N}_2} \frac{^{28}\text{N}_2^+ + ^{44}\text{CO}_2^{++}}{^{20}\text{Ne}^+ + ^{40}\text{Ar}^{++}}}{^{20}\text{Ne}^+ + ^{40}\text{Ar}^{++}}\right)_{\text{SA}}}{\left(\frac{^{22}\text{Ne}^+ + \alpha_{\text{N}_2} \frac{^{28}\text{N}_2^+ + ^{44}\text{CO}_2^{++}}{^{20}\text{Ne}^+ + ^{40}\text{Ar}^{++}}}{^{20}\text{Ne}^+ + ^{40}\text{Ar}^{++}}\right)_{\text{ST}}} \quad (18)$$

Here the “22” represents all of the ions that are collected by the mass 22 Faraday cup, and the same for “20”.

5.2.2. Ricochet $^{28}\text{N}_2$ on ^{22}Ne interference correction

α_{N_2} is the fraction of the mass 28 beam that interferes at mass 22, and its updated value from Sep 18, 2017 is $1/105,700 = 0.00000946$. The derived equation is:

$$q_{N_2_corr} \equiv \frac{\left(\frac{^{22}\text{Ne}^+ + ^{44}\text{CO}_2^{++}}{^{20}\text{Ne}^+ + ^{40}\text{Ar}^{++}}\right)_{SA}}{\left(\frac{^{22}\text{Ne}^+ + ^{44}\text{CO}_2^{++}}{^{20}\text{Ne}^+ + ^{40}\text{Ar}^{++}}\right)_{ST}} = q_{PIS_corr} \left[\frac{1 + \alpha_{N_2} \left(\frac{rR_{28N_2^+}_{ST}}{^{22}_{ST}} \right)}{1 + \alpha_{N_2} \left(\frac{rR_{28N_2^+}_{SA}}{^{22}_{SA}} \right)} \right] \quad (19)$$

$\frac{rR_{28N_2^+}_{SA}}{^{22}_{SA}}$ is the raw ratio measurement of mass 28 to mass 22, measured by the peak jumping method.

5.2.3. Doubly-charged $^{44}\text{CO}_2$ on singly-charged ^{22}Ne isobaric interference correction

The next correction is the doubly-charged isobaric interference correction for $^{44}\text{CO}_2/^{22}\text{Ne}$.

$$^{44}\text{CO}_2^{++} = \alpha_{CO_2} ^{44}\text{CO}_2^+ \quad (20)$$

α_{CO_2} is the fraction of the mass 44 beam that becomes doubly-charged and interferes at mass 22

$\left(\frac{m}{z} = 22\right)$ and the updated value from Aug 29, 2017 is 0.013. The derived equation is:

$$q_{CO_2_corr} \equiv \frac{\left(\frac{^{22}\text{Ne}^+}{^{20}\text{Ne}^+ + ^{40}\text{Ar}^{++}}\right)_{SA}}{\left(\frac{^{22}\text{Ne}^+}{^{20}\text{Ne}^+ + ^{40}\text{Ar}^{++}}\right)_{ST}} = q_{N_2_corr} \left[\frac{1 + \left(\frac{\alpha_{CO_2}}{\frac{1}{rR_{44CO_2^+}_{ST}} - \alpha_{CO_2}} \right)}{1 + \left(\frac{\alpha_{CO_2}}{\frac{1}{rR_{44CO_2^+}_{SA}} - \alpha_{CO_2}} \right)} \right] \quad (21)$$

$rR_{\frac{44CO_2^+}{22}}$ is the raw ratio measurement of mass 44 to mass 22, measured by the peak jumping method.

5.2.4. Doubly-charged ^{40}Ar on singly-charged ^{20}Ne isobaric interference correction

The last correction is for doubly-charged isobaric interference from ^{40}Ar on ^{20}Ne , so

$$q_{Ar_corr} \equiv \frac{\left(\frac{^{22}\text{Ne}_{SA}^+}{^{20}\text{Ne}_{SA}^+}\right)}{\left(\frac{^{22}\text{Ne}_{ST}^+}{^{20}\text{Ne}_{ST}^+}\right)} = q_{true} \text{ and } \delta^{22}\text{Ne}_{true} = (q_{true} - 1) \times 1000\text{‰} \quad (22)$$

Mathematically, Ar interferes with $\delta^{22}\text{Ne}$ in the denominator on both sample and standard, so the correction equation needs to be inverted during the derivation. The outcome is:

$$\frac{1}{q_{Ar_corr}} = \frac{1}{q_{CO_2_corr}} - \frac{^{22}\text{Ne}_{ST}^+}{^{20}\text{Ne}_{ST}^+} \alpha_{Ar} \left(\frac{true_{^{40}\text{Ar}_{SA}^+}}{^{22}\text{Ne}_{SA}^+} - \frac{true_{^{40}\text{Ar}_{ST}^+}}{^{22}\text{Ne}_{ST}^+} \right) \quad (23)$$

α_{Ar} is the fraction of the mass 40 beam that becomes doubly-charged and interferes at mass 20

$\left(\frac{m}{z} = 20\right)$, which is not measured directly. Instead, it is combined with the term $\frac{^{22}\text{Ne}_{ST}^+}{^{20}\text{Ne}_{ST}^+}$ and the

product $\frac{^{22}\text{Ne}_{ST}^+}{^{20}\text{Ne}_{ST}^+} \alpha_{Ar}$ is the slope of the Ar chem-slope experiment.

$$true_{\frac{^{40}\text{Ar}_{SA}^+}{^{22}\text{Ne}_{SA}^+}} = rR_{\frac{^{40}\text{Ar}_{SA}^+}{^{22}\text{Ne}_{SA}^+}} \left[1 + \left(\frac{\frac{\alpha_{CO_2}}{1}}{\frac{rR_{\frac{^{44}\text{CO}_2^+}{^{22}\text{SA}}}}{^{22}\text{SA}} - \alpha_{CO_2}}} \right) \right] \quad (24)$$

$$true_{\frac{^{40}\text{Ar}_{ST}^+}{^{22}\text{Ne}_{ST}^+}} = \frac{1}{q_{CO_2_corr}} rR_{\frac{^{40}\text{Ar}_{ST}^+}{^{22}\text{Ne}_{ST}^+}} \left[1 + \left(\frac{\frac{\alpha_{CO_2}}{1}}{\frac{rR_{\frac{^{44}\text{CO}_2^+}{^{22}\text{ST}}}}{^{22}\text{ST}} - \alpha_{CO_2}}} \right) \right] \quad (25)$$

$rR_{\frac{40}{22}Ar^+}$ is the raw ratio measurement of mass 40 to mass 22, measured by the peak

jumping method.

5.3. La Jolla Air as the standard

The precision of neon isotope measurements from LJA improved, in a second LJA campaign, after making the above modifications to the method. Figure 24a shows LJA $\delta^{22}\text{Ne}$ before and after interference corrections. The external precision before corrections are applied is low ($\sigma = 1.17\%$) as expected. With the more precise interfering fractions (α_{N_2} and α_{CO_2}), Ar chem-slope, and exact mathematical interference correction, the external precision of 10 aliquots improved significantly ($\sigma = 0.023\%$), which satisfies the project's overall requirement to obtain a precision of 0.03%. With these results, we show that we are able to measure neon isotopes at high precision for LJA, and therefore we are ready to measure SGA.

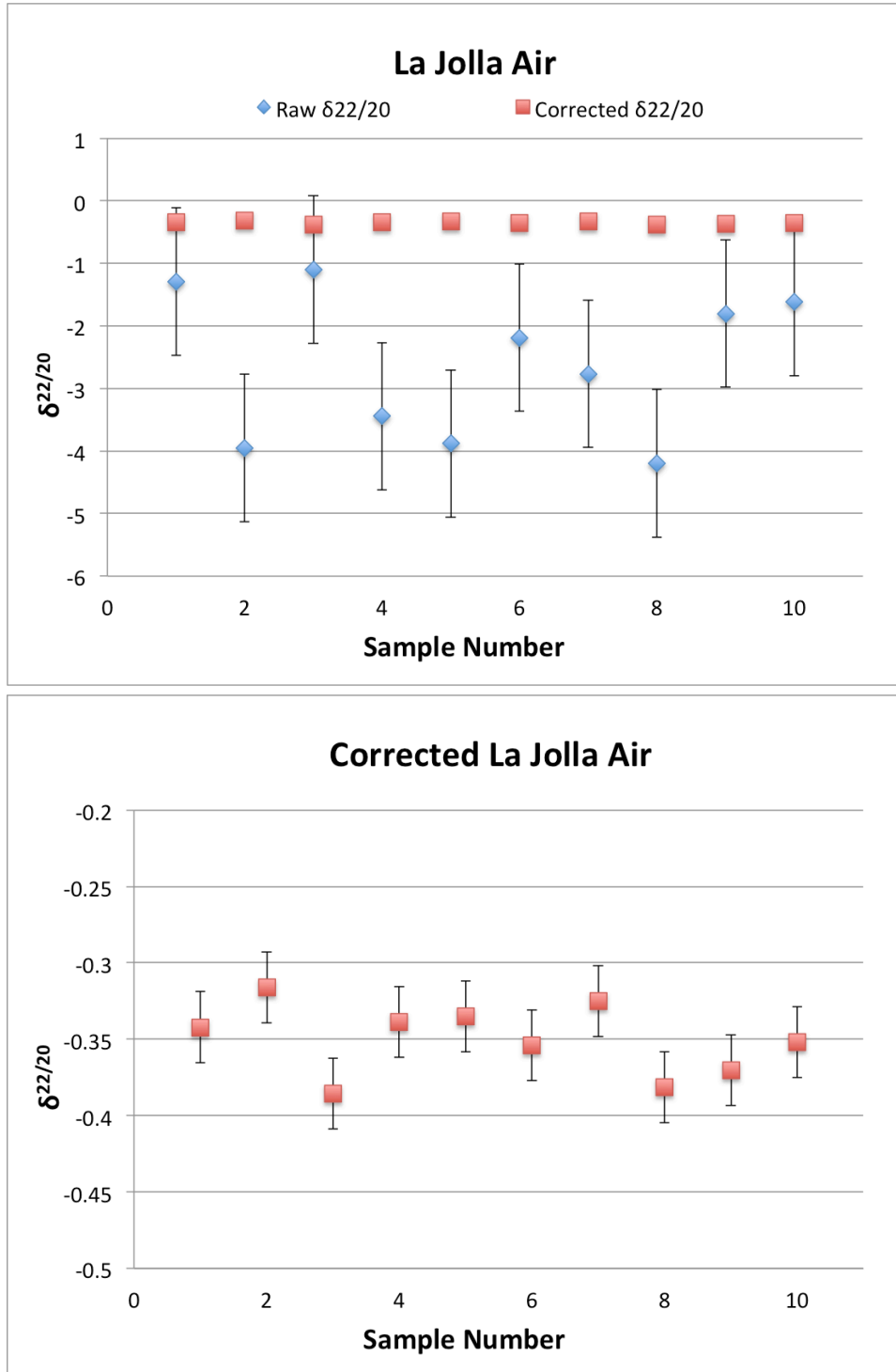


Figure 24: Results of LJA. a) Raw and Corrected La Jolla Air. b) Expanded y-axis to show the corrected La Jolla Air in detail. The exact mathematical corrections have improved the external precision and satisfy the requirement of 0.03 ‰. (n = 10, mean = -0.35, $\sigma = 0.023\text{‰}$)

5.4. Surface Greenland air

Despite the adjustments to the method and corrections, the problem that the surface SFA measurements are different from LJA persists. Two out of six extractions are free of any potential mistakes, and yet the $\delta^{22}\text{Ne}$ values are -0.47 and -0.96 ‰, which are both much more negative than the average LJA $\delta^{22}\text{Ne}$ (-0.35 ‰).

5.5. Discussion: Why surface Greenland air \neq La Jolla air?

5.5.1. Different pressure and vessel?

The methodological differences between SGA and LJA extractions were the pressure of the air sample, and the vessels that SGA and LJA were collected with. LJA was collected at 1 atm in a 2L-glass flask with Louwers-Hapert valves, whereas the ~ 2 atm SGA was collected in 35L-stainless steel Essex tanks with a 4H valve.

To probe potential effects of these differences, Alan Seltzer gettered an 80 ml aliquot of air directly from the Essex tank and measured $\delta^{40}\text{Ar}$ precisely. The result is 0.001 ‰ different from $\delta^{40}\text{Ar}$ of LJA, an insignificant difference, which means $\delta^{40}\text{Ar}$ of SGA is essentially the same as LJA. This rules out the hypothesis that something about the Essex tank causes fractionation of neon. Furthermore, Sarah Shackleton recently measured high-precision Ar, Kr, and Xe isotopes on all SGA tanks, finding excellent reproducibility and results that conform to expectations, so it seems highly unlikely that something is wrong with the SGA samples. Although we only extracted one aliquot, the Ar isotope measurement gave us a hint that the neon isotope fractionation of 4 to 6 ‰ is probably not caused by the 4H valve, unless neon behaves very differently from argon during the expansion. It seems unlikely that neon would fractionate so much (in the ‰ range) when argon does not.

Instead of making the SGA extraction mimic the LJA, we tried to make LJA like SGA by pumping LJA into a pre-evacuated Essex tank with pressure of about 1.5 atm. Six aliquots of LJA from this Essex tank were extracted directly from the tank, and the $\delta^{22}\text{Ne}$ values have a range from -4 to -7 ‰. This fractionation is so large that it cannot simply be thermal fractionation due to expansion of air, and temperature sensors attached to two opposite sides of the tank verify that there is no large temperature gradient.

5.5.2. Thermal expansion?

To make the SGA extraction exactly the same as LJA, we first expanded SGA into a 2L-glass flask to eliminate the possibility of fractionation due to different pressure and different valves. The problem seemed to get worse because the two $\delta^{22}\text{Ne}$ measurements are -6.16 ‰ and -4.86 ‰. We could not make a conclusion with only two measurements, and there are more tests needed to confirm that there is no fractionation due to insufficient equilibration time between a 35L tank and a 2L flask, and thermal fractionation during expansion. We may investigate this further in the future.

5.5.3. Mass spectrometer changed?

After investigating possible issues from the vacuum line setting and the air vessels, we looked carefully at the mass spectrometer again. We realized that the box and trap values have changed, but we do not know when it changed. It is possible that the filament changes after being used for a period of time, and the measurements were far off from LJA after a new filament was replaced. The filament might have changed when we transitioned from LJA to SGA and began to get very negative and irreproducible values.

6. Conclusion

6.1. Achievements

Neon extraction from air has been successful for LJA with external precision of 0.023 ‰, and it appears possible to get suitable SGA measurements on the next attempt. We successfully separated neon and argon gases using a 5Å mol-sieve at 77K, and derived precise mathematical interference corrections for doubly charged argon and carbon dioxide, and ricochet nitrogen.

6.2. Next attempt

The next step of this method development will be to demonstrate that we can achieve high precision for LJA $\delta^{22}\text{Ne}$ measurements from the Essex Tank (denoted LJA_{ET}). There are three possible scenarios: (1) If $\text{LJA} = \text{LJA}_{\text{ET}}$ and $\text{SGA} = \text{LJA}_{\text{ET}}$, then the source of the mass spectrometer has changed, which changed the fraction of doubly charged for $^{44}\text{CO}_2$ and ^{40}Ar , and $^{28}\text{N}_2$ ricochet. (2) If $\text{LJA} \neq \text{LJA}_{\text{ET}}$, then the geometry and pressure of the vessel does matter. We will need to further investigate the physics of this matter. (3) If $\text{SFA} \neq \text{LJA}_{\text{ET}}$, then there is neon fractionation due to an unknown sampling error in the field or during previous extractions from other measurements in the Scripps Noble Gas Isotope Lab.

After the neon isotope ratio of the firm air is measured, we hope to find out more details of how and why gases leak out of ice, and further understand how ice-cores trap ancient air. With more precise climate reconstruction, better models and predictions of future climate can be made.

7. Appendix

7.1. Derivation of approximate mathematical corrections

Ar doubly-charged interference correction derivation:

Known:

$$\frac{{}^{22}\text{Ne}^+}{{}^{20}\text{Ne}^+} = \frac{1}{10}; \frac{{}^{40}\text{Ar}^{++}}{{}^{40}\text{Ar}^+} = \frac{1}{7}$$

$$\delta^{22}\text{Ne}_{obs} = \left[\frac{\left(\frac{{}^{22}\text{Ne}_{SA}^+}{{}^{20}\text{Ne}_{SA}^+ + {}^{40}\text{Ar}_{SA}^{++}} \right)}{\left(\frac{{}^{22}\text{Ne}_{ST}^+}{{}^{20}\text{Ne}_{ST}^+ + {}^{40}\text{Ar}_{ST}^{++}} \right)} - 1 \right] \times 1000\text{‰}$$

Divide by $\frac{{}^{20}\text{Ne}_{ST}^+}{{}^{20}\text{Ne}_{ST}^+}$

$$\delta^{22}\text{Ne}_{obs} = \left[\frac{\left(\frac{\frac{{}^{22}\text{Ne}_{SA}^+}{{}^{20}\text{Ne}_{ST}^+}}{\frac{{}^{20}\text{Ne}_{SA}^+ + {}^{40}\text{Ar}_{SA}^{++}}{{}^{20}\text{Ne}_{ST}^+}} \right)}{\left(\frac{\frac{{}^{22}\text{Ne}_{ST}^+}{{}^{20}\text{Ne}_{ST}^+}}{\frac{{}^{20}\text{Ne}_{ST}^+ + {}^{40}\text{Ar}_{ST}^{++}}{{}^{20}\text{Ne}_{ST}^+}} \right)} - 1 \right] \times 1000\text{‰}$$

If ${}^{20}\text{Ne}_{SA}^+ = {}^{20}\text{Ne}_{ST}^+$ and ${}^{22}\text{Ne}_{SA}^+ = {}^{22}\text{Ne}_{ST}^+$, then

$$\delta^{22}\text{Ne}_{obs} = \left[\frac{\left(\frac{\frac{{}^{22}\text{Ne}_{ST}^+}{{}^{20}\text{Ne}_{ST}^+}}{\frac{{}^{20}\text{Ne}_{ST}^+ + {}^{40}\text{Ar}_{SA}^{++}}{{}^{20}\text{Ne}_{ST}^+}} \right)}{\left(\frac{\frac{{}^{22}\text{Ne}_{ST}^+}{{}^{20}\text{Ne}_{ST}^+}}{\frac{{}^{20}\text{Ne}_{ST}^+ + {}^{40}\text{Ar}_{ST}^{++}}{{}^{20}\text{Ne}_{ST}^+}} \right)} - 1 \right] \times 1000\text{‰}$$

$$\delta^{22}Ne_{obs} = \left[\frac{\left(\frac{1}{1 + \frac{{}^{40}Ar_{SA}^{++}}{{}^{20}Ne_{ST}^+}} \right)}{\left(\frac{1}{1 + \frac{{}^{40}Ar_{ST}^{++}}{{}^{20}Ne_{ST}^+}} \right)} - 1 \right] \times 1000\text{‰}$$

Assuming there is no Ar in the standard can, $\frac{{}^{40}Ar_{ST}^{++}}{{}^{20}Ne_{ST}^+} = 0$

$$\delta^{22}Ne_{Ar-artifact} = \left[\left(\frac{1}{1 + \frac{{}^{40}Ar_{SA}^{++}}{{}^{20}Ne_{ST}^+}} \right) - 1 \right] \times 1000\text{‰}$$

$$\frac{{}^{40}Ar_{SA}^{++}}{{}^{20}Ne_{ST}^+} = \frac{{}^{40}Ar_{SA}^{++}}{10 \text{ } {}^{22}Ne_{ST}^+} = \frac{1}{7} \left(\frac{{}^{40}Ar_{SA}^+}{{}^{10} \text{ } {}^{22}Ne_{ST}^+} \right)$$

CO₂ doubly-charged interference correction and N₂ ricochet interference correction are simple so no derivation is needed.

7.2. Derivation of more precise mathematical corrections

More precise N₂ ricochet interference correction derivation:

$$22_{ST} = {}^{22}\text{Ne}_{ST}^+ + {}^{44}\text{CO}_{2ST}^{++}$$

$$22_{SA} = {}^{22}\text{Ne}_{SA}^+ + {}^{44}\text{CO}_{2SA}^{++}$$

$$20_{ST} = {}^{20}\text{Ne}_{ST}^+ + {}^{40}\text{Ar}_{ST}^{++}$$

$$20_{SA} = {}^{20}\text{Ne}_{SA}^+ + {}^{40}\text{Ar}_{SA}^{++}$$

$\alpha_{N_2} \equiv$ fraction of the mass 28 beam that interferes at mass 22

$$q_{PIS-corr} = \frac{\left(\frac{22_{SA} + \alpha_{N_2} {}^{28}\text{N}_{2SA}^+}{20_{SA}} \right)}{\left(\frac{22_{ST} + \alpha_{N_2} {}^{28}\text{N}_{2ST}^+}{20_{ST}} \right)}$$

$$q_{PIS-corr} \left(\frac{22_{ST}}{20_{ST}} \right) + q_{PIS-corr} \frac{\alpha_{N_2} {}^{28}\text{N}_{2ST}^+}{20_{ST}} = \frac{22_{SA}}{20_{SA}} + \frac{\alpha_{N_2} {}^{28}\text{N}_{2SA}^+}{20_{SA}}$$

divide by $\frac{20_{SA}}{20_{ST}}$

$$q_{PIS-corr} + q_{PIS-corr} \frac{\alpha_{N_2} {}^{28}\text{N}_{2ST}^+}{22_{ST}} = \frac{\left(\frac{22_{SA}}{20_{SA}} \right)}{\left(\frac{22_{ST}}{20_{ST}} \right)} + \frac{\left(\frac{\alpha_{N_2} {}^{28}\text{N}_{2SA}^+}{20_{SA}} \right)}{\left(\frac{22_{ST}}{20_{ST}} \right)}$$

$$q_{N_2-corr} \equiv \frac{\left(\frac{22_{SA}}{20_{SA}} \right)}{\left(\frac{22_{ST}}{20_{ST}} \right)}$$

Substitute $q_{N_2-corr} = \frac{\left(\frac{22_{SA}}{20_{SA}} \right)}{\left(\frac{22_{ST}}{20_{ST}} \right)}$ into previous equation

$$q_{PIS-corr} + q_{PIS-corr} \alpha_{N_2} \left(\frac{{}^{28}\text{N}_{2ST}^+}{22_{ST}} \right) = q_{N_2-corr} + \alpha_{N_2} {}^{28}\text{N}_{2SA} \left(\frac{q_{N_2-corr}}{22_{SA}} \right)$$

Rearrange terms

$$q_{N_2-corr} = q_{PIS-corr} \left[\frac{1 + \alpha_{N_2} \left(\frac{{}^{28}N_{2ST}^+}{22_{ST}} \right)}{1 + \alpha_{N_2} \left(\frac{{}^{28}N_{2SA}^+}{22_{SA}} \right)} \right]$$

More precise CO₂ doubly charged interference derivation:

$\alpha_{CO_2} \equiv$ fraction of the mass 44 beam that becomes doubly-charged and interferes at mass 22 ($\frac{m}{2} = 22$)

$$q_{N_2-corr} = \frac{\left(\frac{22_{SA}}{20_{SA}} \right)}{\left(\frac{22_{ST}}{20_{ST}} \right)} = \frac{\left(\frac{{}^{22}Ne_{SA}^+ + \alpha_{CO_2} {}^{44}CO_{2SA}^+}{20_{SA}} \right)}{\left(\frac{{}^{22}Ne_{ST}^+ + \alpha_{CO_2} {}^{44}CO_{2ST}^+}{20_{ST}} \right)}$$

$$q_{CO_2-corr} \equiv \frac{\left(\frac{{}^{22}Ne_{SA}^+}{20_{SA}} \right)}{\left(\frac{{}^{22}Ne_{ST}^+}{20_{ST}} \right)}$$

$$q_{N_2-corr} \left(\frac{{}^{22}Ne_{ST}^+}{20_{ST}} \right) + q_{N_2-corr} \alpha_{CO_2} \left(\frac{{}^{44}CO_{ST}^+}{20_{ST}} \right) = \frac{{}^{22}Ne_{SA}^+}{20_{SA}} + \alpha_{CO_2} \left(\frac{{}^{44}CO_{2SA}^+}{20_{SA}} \right)$$

Rearrange terms

$$q_{N_2-corr} \left(\frac{{}^{22}Ne_{ST}^+}{20_{ST}} \right) = \frac{{}^{22}Ne_{SA}^+}{20_{SA}} + \alpha_{CO_2} \left(\frac{{}^{44}CO_{2SA}^+}{20_{SA}} \right) - q_{N_2-corr} \alpha_{CO_2} \left(\frac{{}^{44}CO_{ST}^+}{20_{ST}} \right)$$

Divide by $\frac{{}^{22}Ne_{ST}^+}{20_{ST}}$

$$q_{N_2-corr} = \frac{\left(\frac{{}^{22}Ne_{SA}^+}{20_{SA}} \right)}{\left(\frac{{}^{22}Ne_{ST}^+}{20_{ST}} \right)} + \alpha_{CO_2} \left[\frac{\left(\frac{{}^{44}CO_{2SA}^+}{20_{SA}} \right)}{\left(\frac{{}^{22}Ne_{ST}^+}{20_{ST}} \right)} - q_{N_2-corr} \frac{\left(\frac{{}^{44}CO_{ST}^+}{20_{ST}} \right)}{\left(\frac{{}^{22}Ne_{ST}^+}{20_{ST}} \right)} \right]$$

Rearrange terms and substitute $q_{CO_2-corr} = \frac{\left(\frac{^{22}Ne_{SA}^+}{^{20}SA}\right)}{\left(\frac{^{22}Ne_{ST}^+}{^{20}ST}\right)}$

$$q_{N_2-corr} = q_{CO_2-corr} + \alpha_{CO_2} \left[q_{CO_2-corr} \left(\frac{^{44}CO_{2SA}^+}{^{22}Ne_{SA}^+} \right) - q_{N_2-corr} \left(\frac{^{44}CO_{ST}^+}{^{22}Ne_{ST}^+} \right) \right]$$

$$q_{N_2-corr} \left[1 + \alpha_{CO_2} \left(\frac{^{44}CO_{ST}^+}{^{22}Ne_{ST}^+} \right) \right] = q_{CO_2-corr} \left[1 + \alpha_{CO_2} \left(\frac{^{44}CO_{2SA}^+}{^{22}Ne_{SA}^+} \right) \right]$$

$$q_{CO_2-corr} = q_{N_2-corr} \frac{\left[1 + \alpha_{CO_2} \left(\frac{^{44}CO_{ST}^+}{^{22}Ne_{ST}^+} \right) \right]}{\left[1 + \alpha_{CO_2} \left(\frac{^{44}CO_{2SA}^+}{^{22}Ne_{SA}^+} \right) \right]}$$

$$\text{Since } rR_{^{44}CO_{2ST}^+} = \frac{^{44}CO_{2ST}^+}{^{22}Ne_{ST}^+ + ^{44}CO_{2ST}^+} = \frac{^{44}CO_{2ST}^+}{^{22}Ne_{ST}^+ + \alpha_{CO_2} ^{44}CO_{2ST}^+} = \frac{1}{\left(\frac{^{22}Ne_{ST}^+}{^{44}CO_{2ST}^+}\right) + \alpha_{CO_2}}$$

$$\text{so } \frac{^{22}Ne_{ST}^+}{^{44}CO_{2ST}^+} + \alpha_{CO_2} = \frac{1}{rR_{^{44}CO_{2ST}^+}} \text{ and } \frac{^{22}Ne_{ST}^+}{^{44}CO_{2ST}^+} = \frac{1}{rR_{^{44}CO_{2ST}^+}} - \alpha_{CO_2}$$

$$\text{Then } \frac{^{44}CO_{2ST}^+}{^{22}Ne_{ST}^+} = \frac{1}{\frac{1}{rR_{^{44}CO_{2ST}^+}} - \alpha_{CO_2}}$$

Similar equation can be derived for $\frac{^{44}CO_{2SA}^+}{^{22}Ne_{SA}^+}$

$$\text{Substitute } \frac{^{44}CO_{2ST}^+}{^{22}Ne_{ST}^+} = \frac{1}{\frac{1}{rR_{^{44}CO_{2ST}^+}} - \alpha_{CO_2}} \text{ and } \frac{^{44}CO_{2SA}^+}{^{22}Ne_{SA}^+} = \frac{1}{\frac{1}{rR_{^{44}CO_{2SA}^+}} - \alpha_{CO_2}} \text{ for}$$

$$q_{CO_2-corr} = q_{N_2-corr} \frac{\left[1 + \alpha_{CO_2} \left(\frac{^{44}CO_{ST}^+}{^{22}Ne_{ST}^+} \right) \right]}{\left[1 + \alpha_{CO_2} \left(\frac{^{44}CO_{2SA}^+}{^{22}Ne_{SA}^+} \right) \right]}$$

$$\begin{aligned}
q_{CO_2-corr} &= q_{N_2-corr} \frac{\left[1 + \alpha_{CO_2} \left(\frac{1}{\frac{1}{\frac{rR^{44}CO_2^+_{2ST}}{22_{ST}}} - \alpha_{CO_2}}} \right) \right]}{\left[1 + \alpha_{CO_2} \left(\frac{1}{\frac{1}{\frac{rR^{44}CO_2^+_{2SA}}{22_{SA}}} - \alpha_{CO_2}}} \right) \right]} \\
&= q_{N_2-corr} \frac{\left[1 + \left(\frac{\alpha_{CO_2}}{\frac{1}{\frac{rR^{44}CO_2^+_{2ST}}{22_{ST}}} - \alpha_{CO_2}}} \right) \right]}{\left[1 + \left(\frac{\alpha_{CO_2}}{\frac{1}{\frac{rR^{44}CO_2^+_{2SA}}{22_{SA}}} - \alpha_{CO_2}}} \right) \right]}
\end{aligned}$$

More precise Ar doubly charged interference correction derivation:

$\alpha_{Ar} \equiv$ fraction of the mass 40 beam that becomes doubly-charged and interferes at mass 20 ($\frac{m}{z} = 20$)

$$q_{CO_2-corr} = \frac{\left(\frac{{}^{22}Ne^+_{SA}}{20_{SA}} \right)}{\left(\frac{{}^{22}Ne^+_{ST}}{20_{ST}} \right)} = \frac{\left(\frac{{}^{22}Ne^+_{SA}}{{}^{20}Ne^+_{SA} + {}^{40}Ar^{++}_{SA}} \right)}{\left(\frac{{}^{22}Ne^+_{ST}}{{}^{20}Ne^+_{ST} + {}^{40}Ar^{++}_{ST}} \right)} = \frac{\left(\frac{{}^{22}Ne^+_{SA}}{{}^{20}Ne^+_{SA} + \alpha_{Ar} {}^{40}Ar^+_{SA}} \right)}{\left(\frac{{}^{22}Ne^+_{ST}}{{}^{20}Ne^+_{ST} + \alpha_{Ar} {}^{40}Ar^+_{ST}} \right)}$$

Invert q_{CO_2-corr}

$$\frac{1}{q_{CO_2-corr}} = \frac{\left(\frac{{}^{22}Ne^+_{ST}}{{}^{20}Ne^+_{ST} + \alpha_{Ar} {}^{40}Ar^+_{ST}} \right)}{\left(\frac{{}^{22}Ne^+_{SA}}{{}^{20}Ne^+_{SA} + \alpha_{Ar} {}^{40}Ar^+_{SA}} \right)}$$

$$\left(\frac{1}{q_{CO_2-corr}}\right)\left(\frac{{}^{20}Ne_{ST}^+}{{}^{22}Ne_{ST}^+}\right) + \left(\frac{1}{q_{CO_2-corr}}\right)\left(\frac{\alpha_{Ar} {}^{40}Ar_{ST}^+}{{}^{22}Ne_{ST}^+}\right) = \frac{{}^{20}Ne_{SA}^+}{{}^{22}Ne_{SA}^+} + \frac{\alpha_{Ar} {}^{40}Ar_{SA}^+}{{}^{22}Ne_{SA}^+}$$

Rearrange terms

$$\left(\frac{1}{q_{CO_2-corr}}\right)\left(\frac{{}^{20}Ne_{ST}^+}{{}^{22}Ne_{ST}^+}\right) = \frac{{}^{20}Ne_{SA}^+}{{}^{22}Ne_{SA}^+} + \alpha_{Ar} \left[\frac{{}^{40}Ar_{SA}^+}{{}^{22}Ne_{SA}^+} - \left(\frac{1}{q_{CO_2-corr}}\right)\left(\frac{{}^{40}Ar_{ST}^+}{{}^{22}Ne_{ST}^+}\right) \right]$$

Divide by $\frac{{}^{20}Ne_{ST}^+}{{}^{22}Ne_{ST}^+}$

$$\frac{1}{q_{CO_2-corr}} = \frac{\left(\frac{{}^{20}Ne_{SA}^+}{{}^{22}Ne_{SA}^+}\right)}{\left(\frac{{}^{20}Ne_{ST}^+}{{}^{22}Ne_{ST}^+}\right)} + \frac{\alpha_{Ar}}{\left(\frac{{}^{20}Ne_{ST}^+}{{}^{22}Ne_{ST}^+}\right)} \left[\frac{{}^{40}Ar_{SA}^+}{{}^{22}Ne_{SA}^+} - \left(\frac{1}{q_{CO_2-corr}}\right)\left(\frac{{}^{40}Ar_{ST}^+}{{}^{22}Ne_{ST}^+}\right) \right]$$

$$\frac{1}{q_{Ar-corr}} \equiv \frac{\left(\frac{{}^{20}Ne_{SA}^+}{{}^{22}Ne_{SA}^+}\right)}{\left(\frac{{}^{20}Ne_{ST}^+}{{}^{22}Ne_{ST}^+}\right)}$$

Substitute $\frac{1}{q_{Ar-corr}} = \frac{\left(\frac{{}^{20}Ne_{SA}^+}{{}^{22}Ne_{SA}^+}\right)}{\left(\frac{{}^{20}Ne_{ST}^+}{{}^{22}Ne_{ST}^+}\right)}$ in $\frac{1}{q_{CO_2-corr}}$ and rearrange terms

$$\frac{1}{q_{CO_2-corr}} = \frac{1}{q_{Ar-corr}} + \alpha_{Ar} \left(\frac{{}^{22}Ne_{ST}^+}{{}^{20}Ne_{ST}^+} \right) \left[\frac{{}^{40}Ar_{SA}^+}{{}^{22}Ne_{SA}^+} - \left(\frac{1}{q_{CO_2-corr}}\right)\left(\frac{{}^{40}Ar_{ST}^+}{{}^{22}Ne_{ST}^+}\right) \right]$$

$$\frac{1}{q_{Ar-corr}} = \frac{1}{q_{CO_2-corr}} - \alpha_{Ar} \left(\frac{{}^{22}Ne_{ST}^+}{{}^{20}Ne_{ST}^+} \right) \left[\frac{{}^{40}Ar_{SA}^+}{{}^{22}Ne_{SA}^+} - \left(\frac{1}{q_{CO_2-corr}}\right)\left(\frac{{}^{40}Ar_{ST}^+}{{}^{22}Ne_{ST}^+}\right) \right]$$

$$rR_{\frac{{}^{40}Ar_{ST}^+}{{}^{22}Ne_{ST}^+}} = \frac{{}^{40}Ar_{ST}^+}{{}^{22}Ne_{ST}^+ + \alpha_{CO_2} {}^{44}CO_{2ST}^+}$$

$$rR_{\frac{{}^{40}Ar_{ST}^+}{{}^{22}Ne_{ST}^+}} \left({}^{22}Ne_{ST}^+ + \alpha_{CO_2} {}^{44}CO_{2ST}^+ \right) = {}^{40}Ar_{ST}^+$$

Divide by ${}^{22}Ne_{SA}^+$ and rearrange terms

$$\frac{{}^{40}\text{Ar}_{ST}^+}{{}^{22}\text{Ne}_{ST}^+} = rR_{40\text{Ar}_{ST}^+} \left(1 + \alpha_{\text{CO}_2} \frac{{}^{44}\text{CO}_{2ST}^+}{{}^{22}\text{Ne}_{ST}^+} \right) = rR_{40\text{Ar}_{ST}^+} \left[1 + \left(\frac{\alpha_{\text{CO}_2}}{\frac{1}{\frac{rR_{44}\text{CO}_{2ST}^+}{{}^{22}\text{Ne}_{ST}^+}} - \alpha_{\text{CO}_2}}} \right) \right]$$

Similar equation can be derived for $\frac{{}^{40}\text{Ar}_{SA}^+}{{}^{22}\text{Ne}_{SA}^+}$

$$\frac{{}^{40}\text{Ar}_{SA}^+}{{}^{22}\text{Ne}_{SA}^+} = rR_{40\text{Ar}_{SA}^+} \left(1 + \alpha_{\text{CO}_2} \frac{{}^{44}\text{CO}_{2SA}^+}{{}^{22}\text{Ne}_{SA}^+} \right) = rR_{40\text{Ar}_{SA}^+} \left[1 + \left(\frac{\alpha_{\text{CO}_2}}{\frac{1}{\frac{rR_{44}\text{CO}_{2SA}^+}{{}^{22}\text{Ne}_{SA}^+}} - \alpha_{\text{CO}_2}}} \right) \right]$$

Substitute $\frac{{}^{40}\text{Ar}_{ST}^+}{{}^{22}\text{Ne}_{ST}^+} = rR_{40\text{Ar}_{ST}^+} \left[1 + \left(\frac{\alpha_{\text{CO}_2}}{\frac{1}{\frac{rR_{44}\text{CO}_{2ST}^+}{{}^{22}\text{Ne}_{ST}^+}} - \alpha_{\text{CO}_2}}} \right) \right]$ and

$$\frac{{}^{40}\text{Ar}_{SA}^+}{{}^{22}\text{Ne}_{SA}^+} = rR_{40\text{Ar}_{SA}^+} \left[1 + \left(\frac{\alpha_{\text{CO}_2}}{\frac{1}{\frac{rR_{44}\text{CO}_{2SA}^+}{{}^{22}\text{Ne}_{SA}^+}} - \alpha_{\text{CO}_2}}} \right) \right] \text{ in } \frac{1}{q_{\text{Ar-corr}}}$$

$$\frac{1}{q_{\text{Ar-corr}}} = \frac{1}{q_{\text{CO}_2\text{-corr}}} - \frac{{}^{22}\text{Ne}_{ST}^+}{{}^{20}\text{Ne}_{ST}^+} \alpha_{\text{Ar}} \left\{ rR_{40\text{Ar}_{SA}^+} \left[1 + \left(\frac{\alpha_{\text{CO}_2}}{\frac{1}{\frac{rR_{44}\text{CO}_{2SA}^+}{{}^{22}\text{Ne}_{SA}^+}} - \alpha_{\text{CO}_2}}} \right) \right] - \frac{1}{q_{\text{CO}_2\text{-corr}}} rR_{40\text{Ar}_{ST}^+} \left[1 + \right. \right.$$

$$\left. \left. \left(\frac{\alpha_{\text{CO}_2}}{\frac{1}{\frac{rR_{44}\text{CO}_{2ST}^+}{{}^{22}\text{Ne}_{ST}^+}} - \alpha_{\text{CO}_2}}} \right) \right] \right\}$$

$$q_{\text{Ar-corr}} = q_{\text{true}}$$

$$\delta^{22}\text{Ne}_{\text{true}} = (q_{\text{true}} - 1) \times 1000\text{‰}$$

References

- Barnola, J. M., D Raynaud, Y. S. Korotkevich, and C. Lorius. 1987. "Vostok Ice Core Provides 160,000-Year Record of Atmospheric CO₂." *Nature* 329 (1).
- Battle, M., M. Bender, T. Sowers, P. P. Tans, J. H. Butler, J. W. Elkins, J. T. Ellis, T. Conway, N. Zhang, p. Lang, and A.D. Clark. 1996. "Atmospheric Gas Concentrations over the Past Century Measured in Air from Firn at the South Pole." *Nature*. doi:10.1038/383231a0.
- Battle, M. O., J. P. Severinghaus, E. D. Sofen, D. Plotkin, A. J. Orsi, M. Aydin, S. A. Montzka, T. Sowers, and P. P. Tans. 2011. "Controls on the Movement and Composition of Firn Air at the West Antarctic Ice Sheet Divide." *Atmospheric Chemistry and Physics* 11 (21): 11007–21. doi:10.5194/acp-11-11007-2011.
- Bender, M L, Todd Sowers, and Edward J Brook. 1997. "Gases in Ice Cores." *Proceedings of the National Academy of Sciences USA* 94 (16): 8343–49. doi:10.1073/pnas.94.16.8343.
- Craig, H, and C C Chou. 1982. "Methane: The Recoed in Polar Ice Cores." *Geophysical Research Letters* 9 (11): 1221–24.
- Etheridge, D M, L P Steele, R L Langenfelds, R J Francey, J M Barnola, and V I Morgan. 1996. "Natural and Anthropogenic Changes in Atmospheric CO₂ over the Last 1000 Years from Air in Antarctic Ice and Firn." *Journal Of Geophysical Research-Atmospheres* 101 (D2): 4115–28. doi:10.1029/95JD03410.
- Huber, C., U. Beyerle, M. Leuenberger, J. Schwander, R. Kipfer, R. Spahni, J. P. Severinghaus, and K. Weiler. 2006. "Evidence for Molecular Size Dependent Gas Fractionation in Firn Air Derived from Noble Gases, Oxygen, and Nitrogen Measurements." *Earth and Planetary Science Letters* 243 (1–2): 61–73. doi:10.1016/j.epsl.2005.12.036.
- Ikeda-Fukazawa, Tomoko, Katsuyuki Kawamura, and Takeo Hondoh. 2004. "Mechanism of Molecular Diffusion in Ice Crystals." *Molecular Simulation* 30 (April 2015): 973–79. doi:10.1080/08927020410001709307.
- Keeling, Ralph F., Stephen C. Piper, and Martin Heimann. 1996. "Global and Hemispheric CO₂ Sinks Deduced from Changes in Atmospheric O₂ Concentration." *Nature*. doi:10.1038/381218a0.
- Kobashi, Takuro, Jeffrey P. Severinghaus, and Kenji Kawamura. 2008. "Argon and Nitrogen Isotopes of Trapped Air in the GISP2 Ice Core during the Holocene Epoch (0-11,500 B.P.): Methodology and Implications for Gas Loss Processes." *Geochimica et Cosmochimica Acta* 72 (19): 4675–86. doi:10.1016/j.gca.2008.07.006.
- Severinghaus, Jeffrey P., and Mark O. Battle. 2006. "Fractionation of Gases in Polar Ice during Bubble Close-off: New Constraints from Firn Air Ne, Kr and Xe Observations." *Earth and Planetary Science Letters* 244 (1–2): 474–500. doi:10.1016/j.epsl.2006.01.032.

Severinghaus, Jeffrey P., Ross Beaudette, Melissa A. Headly, Kendrick Taylor, and Edward J. Brook. 2009. "Oxygen-18 of O₂ Records the Impact of Abrupt Climate Change on the Terrestrial Biosphere." *Science* 324 (5933): 1431–34. doi:10.1126/science.1169473.

Severinghaus, Jeffrey P., Alexi Grachev, Boaz Luz, and Nicolas Caillon. 2003. "A Method for Precise Measurement of Argon 40/36 and Krypton/argon Ratios in Trapped Air in Polar Ice with Applications to Past Firn Thickness and Abrupt Climate Change in Greenland and at Siple Dome, Antarctica." *Geochimica et Cosmochimica Acta* 67 (3): 325–43. doi:10.1016/S0016-7037(02)00965-1.